



UNIVERSIDAD DE CHILE
FACULTAD DE CIENCIAS FÍSICAS Y MATEMÁTICAS
DEPARTAMENTO DE INGENIERÍA ELÉCTRICA

ASTROMETRIC PRECISION SPECTROSCOPY: EXPERIMENTAL DEVELOPMENT
OF A DUAL-FREQUENCY LASER SYNTHESIZER BASED ON AN OPTICAL
FREQUENCY COMB

MEMORIA PARA OPTAR AL TÍTULO DE
INGENIERO CIVIL ELÉCTRICO

TAKY PARVEX PICHADA

PROFESOR GUÍA:
ERNEST ALEXANDER MICHAEL

MIEMBROS DE LA COMISIÓN:
FELIPE ERNESTO BESSER PIMENTEL
NICOLÁS ESTEBAN RAMOS OLIVER

Este trabajo ha sido parcialmente financiado por CONICYT, a través de su fondo ALMA para el desarrollo de la astronomía, proyecto 31140025, QUIMAL, proyecto 1500010, CATA-Basal PFB06 y Fondecyt 1151213

SANTIAGO DE CHILE
2018

RESUMEN DE LA MEMORIA PARA OPTAR
AL TÍTULO DE INGENIERO CIVIL ELÉCTRICO
POR: TAKY PARVEX PICHAIDA
FECHA: 2018
PROF. GUÍA: ERNEST ALEXANDER MICHAEL

ASTROMETRIC PRECISION SPECTROSCOPY: EXPERIMENTAL DEVELOPMENT
OF A DUAL-FREQUENCY LASER SYNTHESIZER BASED ON AN OPTICAL
FREQUENCY COMB

La tecnología de terahercios se encuentra en un estado de desarrollo atrasado con respecto a las tecnologías usadas en las bandas adyacentes, como la óptica infrarroja o la electrónica de microondas. En particular, no se poseen fuentes compactas de radiación que operen dentro esta banda logrando buenos niveles de potencia y amplios rangos de frecuencia. Las útiles propiedades de la radiación de terahercios como su capacidad de detectar moléculas complejas, buena resolución espacial y ser radiación no ionizante, hacen que el desarrollo de tecnología para esta banda sea un área con creciente interés.

En el contexto del desarrollo de una nueva línea de investigación sobre espectroscopía molecular, en el Laboratorio de Terahertz y Astrofotónica de la Universidad de Chile, se realiza este trabajo que consiste en el desarrollo experimental de un sistema láser para la alimentación de fotomezcladores. Este sistema tiene como objetivo la generación de dos señales ópticas de alta estabilidad y coherencia, cuya diferencia de frecuencias puede ser ajustada de forma continua dentro del rango de 10 GHz a 300 GHz.

Para esto, se utiliza un esquema basado en un peine de frecuencias óptico sobre el cual se enclava por inyección un láser de diodos de frecuencia sintonizable. Esto consigue tener una fuente infrarroja de alta precisión dentro de un gran rango. Además, se genera una segunda señal por medio de modulación en amplitud (AM), la cual es sintonizable dentro de un rango igual al espaciado producido por el peine óptico. En conjunto, estas señales logran abarcar un amplio espectro de frecuencias de forma continua sin perder estabilidad ni calidad de las señales.

En este trabajo se logra implementar los subsistemas para la generación de cada una de las señales requeridas y se estudia la capacidad de estos para trabajar dentro del rango deseado. Para la señal generada por enclavamiento por inyección, se logra probar el concepto dentro de un rango reducido, principalmente por falta de un buen sistema de medición de altas frecuencias. Para la señal generada por modulación AM, se logran resultados positivos en todo el rango de diseño. Finalmente, se proponen modificaciones al sistema para mejorar su desempeño.

RESUMEN DE LA MEMORIA PARA OPTAR
AL TÍTULO DE INGENIERO CIVIL ELÉCTRICO
POR: TAKY PARVEX PICHAIDA
FECHA: 2018
PROF. GUÍA: ERNEST ALEXANDER MICHAEL

ASTROMETRIC PRECISION SPECTROSCOPY: EXPERIMENTAL DEVELOPMENT
OF A DUAL-FREQUENCY LASER SYNTHESIZER BASED ON AN OPTICAL
FREQUENCY COMB

Terahertz technology is still in a young phase of development in comparison to the technologies used in adjacent bands, like infrared photonics or microwaves electronics. In particular, there are no compact sources of radiation capable of operating inside this band with good power levels and wide tunability range. The useful properties of terahertz radiation, such as its ability to detect complex molecules, good spatial resolution and its non-ionizing nature, are driving a growing interest in the technological development of this band.

In the Laboratory of Terahertz and Astro-Photonics, at the University of Chile, a new line of research on molecular spectroscopy is being opened. Within this context, this work consists in the experimental development of a laser system to feed a photomixer, with the objective of producing terahertz radiation. This system aims to generate two steady and coherent optical signals, whose frequency difference can be continuously adjusted in the range from 10 GHz to 300 GHz.

To achieve this, one of the signals is generated by injection-locking a wide tunable diode laser to one of the lines of an optical frequency comb. Thanks to this, it manages to synthesize a high precision infrared source within a large range. In addition, a second signal is generated by means of amplitude modulation (AM), which is tunable within a range equal to the spacing between the comb lines. Together, these signals manage to continuously cover a broad spectrum of frequencies without losing stability or quality of the signals.

During this work, it was possible to implement independent systems for the generation of each of the required signals, and the quality of the resulting signals is studied. For the system based in injection locking, it was possible to test the concept only within a reduced range, mainly due to the lack of a proper measurement scheme. For the signal generated with amplitude modulation, good results were obtained through the whole design range. Finally, modifications to the system are proposed, with the objective of improving its performance.

Table of Contents

1. Introduction	1
1.1. General objective	2
1.2. Specific objectives	2
1.3. Overview of this document	2
2. Background Concepts and Contextualization	4
2.1. Terahertz radiation	4
2.1.1. Radiation sources	5
2.2. Lasers	8
2.2.1. Diode lasers	12
2.2.2. Fiber lasers	14
2.3. Laser injection locking	14
2.4. Spectroscopy	16
2.4.1. Terahertz spectroscopy	19
3. Design and Implementation	20
3.1. Wide range, discrete tunable signal	21
3.1.1. Optical frequency comb generator	22
3.1.2. Laser coupling into a single-mode fiber	25
3.1.3. Injection locking	26
3.2. Small range, continuously tunable signal	28
3.2.1. Amplitude modulation	28
3.2.2. Sideband and carrier suppression	29
4. System Evaluation	31
4.1. Discrete tunable signal synthesis	31
4.1.1. YIG oscillator as a reference signal	31
4.1.2. Optical frequency comb generator	35
4.1.3. Injection locking	38
4.2. Continuously tunable signal synthesis	42
4.2.1. Amplitude modulation	42
4.2.2. Sideband and carrier suppression	44
5. Conclusions and Future Work	47
5.1. Conclusions	47
5.2. Future Work	47

Bibliography	50
A. Equipment	54
A.1. Lasers	54
A.1.1. Master laser	54
A.1.2. Slave laser	55
A.2. Optical equipment	56
A.2.1. Optical frequency comb generator	56
A.2.2. Electro-optical modulator	56
A.2.3. Fiber Bragg Grating	57
A.2.4. Optical circulator	58
A.2.5. Manual polarization controller	58
A.2.6. Photodiode	59
A.3. Electrical equipment	59
A.3.1. YIG Oscillator	59
A.3.2. Frequency synthesizer	60
A.3.3. Low noise amplifier	60
B. Operating Instructions	62
B.1. Discrete tunable signal synthesizer	62
B.2. Continuously tunable signal synthesizer	64

List of Tables

2.1. Most common laser active ions, typical host glasses and operating wavelengths.	14
3.1. Power requirements for the YIG and control system.	24
3.2. Most relevant electrical characteristics of the power supply.	25
3.3. Expected attenuation after retrieving the reflected signal from the FBG, considering attenuation produced by the optical circulator.	29
4.1. Mean value and variance of the LSB with the master laser set to different wavelengths.	44
A.1. Koheras AdjustiK E15 optical specifications [35].	54
A.2. New Focus 63289 Velocity tunable diode laser optical specifications.	56
A.3. EOM electrical and optical parameters [36].	57
A.4. Optical circulator specification and test data [37].	58
A.5. DSC 20H photodiode optical and electrical specifications [38].	59
A.6. YIG oscillator specifications.	60
A.7. Frequency synthesizer main specifications.	60
A.8. LNA main specifications.	61

List of Figures

1.1. Number of documents with ‘terahertz’ appearing in the abstract, title or key-word field as a function of time.	1
2.1. Electromagnetic spectrum	4
2.2. THz atmospheric attenuation	6
2.3. THz sources	7
2.4. Photomixing	8
2.5. The three basic processes by which photon-assisted transitions occur.	10
2.6. Laser pumping system	12
2.7. Schematic diagram of a basic laser	13
2.8. Injection locking range	16
2.9. Injection locking phase	17
2.10. Spectral lines observed by Fraunhofer.	17
3.1. Dual frequency synthesizer diagram	21
3.2. Discrete tunable signal synthesizer diagram	22
3.3. YIG oscillator diagram	24
3.4. Optical diagram of the fiber coupling optics. Not to scale.	25
3.5. Fiber-coupling of the diode laser with the cage assembly.	26
3.6. Continuously tunable signal synthesizer diagram	28
3.7. Fiber Bragg grating curves	30
3.8. Continuously tunable signal synthesizer.	30
4.1. YIG drift with and without PLL	32
4.2. YIG output with and without PLL	33
4.3. Sin-to-PLL conversion	33
4.4. Signal after the loop filter.	34
4.5. YIG driven by PLL	34
4.6. OFCG efficiency	35
4.7. OFCG output vs bias voltage	36
4.8. OFCG optical output at different input levels	37
4.9. Setup for measuring the injection locking.	38
4.10. Phases of injection locking	38
4.11. Slave laser with and without injection locking pt. 1	40
4.12. Slave laser with and without injection locking pt. 2	41
4.13. Sidebands and carrier levels vs RF power	42
4.14. Bias voltage effect in amplitude modulation	43

4.15. Sideband suppression	45
4.16. Relative LSB isolation	46
A.1. Koheras AdjustiK E15 laser system.	54
A.2. Velocity 6300 control panel.	55
A.3. Velocity 6300 laser head diagram.	55
A.4. Optical frequency comb generator	57
A.5. Manual fiber polarization controller.	58
A.6. Photodiode and LNA.	59
A.7. Microwave frequency synthesizer.	61

Chapter 1

Introduction

There is growing interest in the electromagnetic radiation that lays in the 100 GHz to 10 THz frequency range, known as *Terahertz radiation*, because of its unique and attractive properties: it has sub-millimeter wavelengths, various common materials are transparent to it, it is non-ionizing and many molecules have a distinctive and unique vibrational and rotational spectra in this region of the electromagnetic spectrum. A clear evidence of this rising interest is shown by Lewis in his review of terahertz sources [1], where he shows that the amount of documents related to terahertz radiation has grown exponentially in the past decades as seen in Figure 1.1. Terahertz radiation can be used to detect hidden guns, explosives or drugs, for biological imaging, to detect pollutants in the atmosphere or to determinate the relative movement and position of other planets [2, 3, 4].

Even with its remarkable properties, the terahertz region remained mostly unexplored during a long time due to the lack of coherent sources of radiation and detectors, therefore receiving the name of ‘terahertz gap’. As this region lays between the microwaves and the infrared regions of the electromagnetic spectrum, there has been efforts to extend the range of the technology deployed in each of these bands to produce terahertz radiation, but microwave electronic sources tend to decrease its output power sharply as frequency increases and classical photonic sources as laser only reach the upper side of the terahertz band. However,

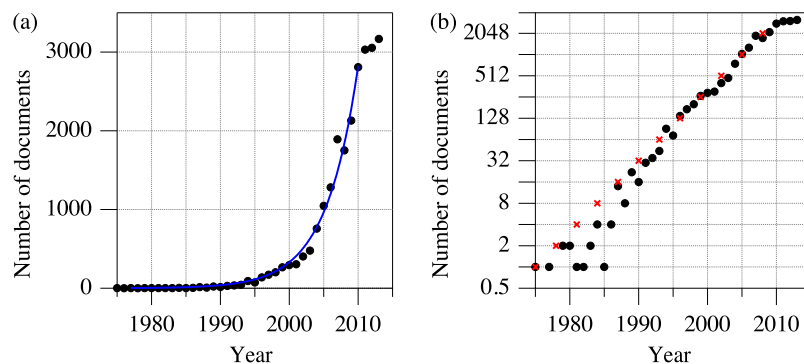


Figure 1.1: Number of documents with ‘terahertz’ appearing in the abstract, title or keyword field as a function of time. (a) Linear-linear scale. (b) Log-linear scale [1].

in the last decades this scenario has changed with the rapid development of new technologies. Nevertheless, there is still the need for more practical systems with reduced volume, higher output powers and wider tuning ranges.

One method to generate coherent terahertz radiation is to combine two laser signals in a photomixer. These devices generate radiation with a frequency equal to the frequency difference between the two incident signals. Photomixers can achieve high tuning range, given that the laser system is tunable, and can be as compact as the laser system used to feed them, but they achieve relative low power. This work, titled “Astrometric Precision Spectroscopy: Experimental Development of a Dual-Frequency Laser Synthesizer Based on an Optical Frequency Comb” is oriented to the development of a tunable dual laser system for a photomixer. With this radiation source, the Terahertz- and Astro-Photonics Lab will open a new research line of high-resolution molecular spectroscopy that could expand the current catalog of known molecular spectra, with direct applications to astronomy and astrometry.

1.1. General objective

Experimental development and characterization of a dual-frequency laser system to be applied in a continuous-wave Terahertz radiation source using photomixers.

1.2. Specific objectives

The dual-frequency laser synthesizer is approached as two independent subsystems. Each of them is implemented and evaluated separately. Therefore, the specific objectives are:

- Implement a wide, discretely tunable laser source based on a diode laser injection-locked to a frequency comb.
- Implement a continuously tunable laser source through amplitude modulation and selective filtering.
- Characterize and evaluate each of the subsystems, selecting appropriate figures of merit for each of them.

1.3. Overview of this document

This document is structured as follows:

- **Chapter 2 - Background Concepts and Contextualization:** An introduction to the most relevant topics that must be known to understand this project.
- **Chapter 3 - Design and Implementation:** Detailed explanation of the design and the implementation process.

- **Chapter 4 - System Evaluation:** Results, analysis and discussion of the implemented system.
- **Chapter 5 - Conclusions and Future Work:** Conclusion about the proposed objectives and recommendations on where to continue this project.

Chapter 2

Background Concepts and Contextualization

2.1. Terahertz radiation

Terahertz radiation, also known as submillimeter waves, terahertz waves, terahertz light, T-rays, T-waves, T-light, T-lux, THz or Tremendously high frequency (THF) [3], is one of the bands of the electromagnetic spectrum. The exact range of frequencies for its definition may vary, but it is usually considered between 100 GHz to 10 THz, or its equivalent wavelength, from 0.03 mm to 3 mm. In astronomy it is more common to refer to this band as the Submillimeter Band with the wavelength range from 0.1 mm to 1 mm. Therefore, it is located between the Infrared and the Microwaves sections of the electromagnetic spectrum and it is considered to overlap with the far-infrared by some sources and authors [5, 2].

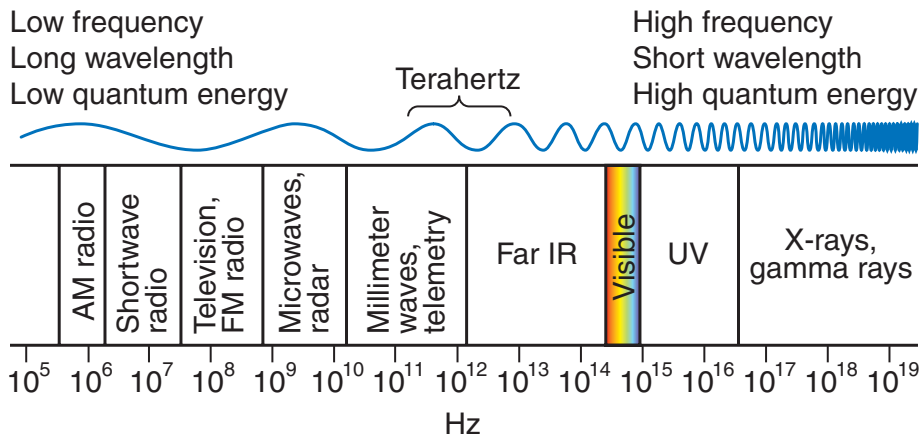


Figure 2.1: The electromagnetic spectrum [2].

Terahertz radiation has an important field of potential applications, most of which are in a young phase of development [6]. There are several interesting properties about this kind of radiation:

- While not as small as the optical, the sub-millimeter wavelength of the terahertz range allows better spatial resolution for imaging than the microwaves regime[6].
- Many materials such as paper, soil, fabric, plastic, and wood are transparent to terahertz radiation [7], while being opaque to visible light. This allows the detection of object hidden to plain sight like guns, illegal drugs or other contraband goods.
- Due to its relative longer wavelength, and thus low photon energy, terahertz radiation is non-ionizing. This means that it is a good alternative to X-rays for medical imaging and chemical analysis of drugs [7] since its safer to the body and less damaging to chemical samples.
- Many molecules have very specific spectra in the terahertz range. Small polar molecules have pure rotational transitions and macromolecules have pure vibrational transitions in this range [6]. These spectra can be used like ‘fingerprints’ to identify those components.

These properties make submillimeter/terahertz radiation of interest for many applications. For example: chemical analysis in the pharmaceutical industry, scanning in homeland security and defense, imaging and measuring in biological systems, monitoring of industrial processes, fast transfer of data, among others.

In particular, vibrational and rotational spectroscopy is one of the fields where terahertz radiation has been most applied to. Analytical chemistry and radio-astronomy have been pushing these developments. Also, highly coherent terahertz radiation can be used as a reference signal for heterodyne detection in radio-astronomical observations [6]. In astronomy, radiation in the terahertz frequency range is of great importance: the peak of radiation density from the cosmic background lies in this region of the electromagnetic spectrum [6] and, as stated by Peter Siegel, “*at least 98 percent of the detectable radiant energy in the universe falls within the terahertz, or far-infrared part of the electromagnetic spectrum*” [8] .

The development of new and better applications of T-rays face two major difficulties: water and oxygen from the atmosphere absorb quickly this kind of radiation, as depicted in Figure 2.2; and the lack of development of compact and affordable terahertz detectors and sources. Until some decades ago, the electronic technology used in microwaves was too slow for the high frequencies of terahertz radiation, while on the other hand typical optical techniques were stalled in the mid-infrared. This is why the terahertz band is also referred as the ‘terahertz gap’.

2.1.1. Radiation sources

In the past decades many different terahertz radiation sources have been developed. Figure 2.3 shows the state of the art in THz radiation sources. Some of the most important are:

Vacuum electronic sources

- **Backward-wave oscillators (BWO):** using an electron gun to shoot an electron beam through a slow-wave structure, BWOs generate stable and powerful (mW) radiation. This radiation can be tuned by changing the voltage of the electron gun and

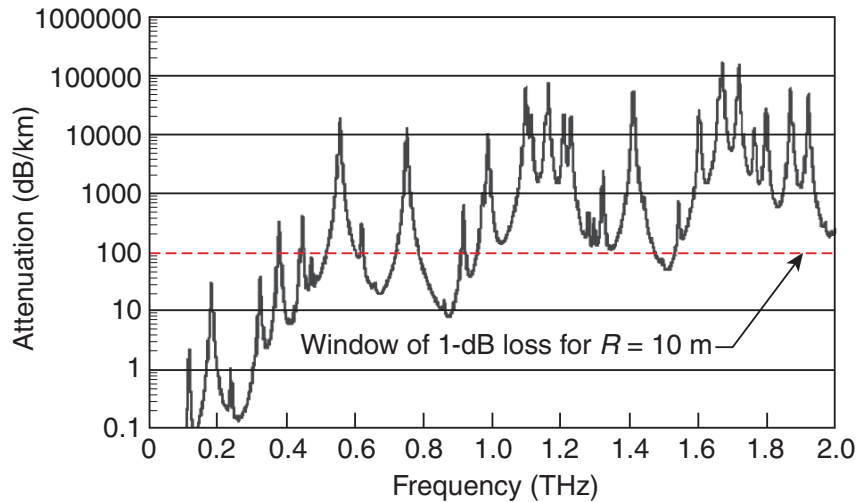


Figure 2.2: THz atmospheric attenuation [2].

proper control systems can be implemented to improve the device's performance. Some common applications are imaging, spectroscopy and as local oscillators in heterodyne detection.

- **Gyrotron:** gyrotrons are capable of generating high-power (kW), terahertz radiation. A gyrotron's operation principle is based on the stimulated cyclotron radiation of electrons oscillating in a strong magnetic field [10].
- **Extended-interaction klystron:** these radiation sources combine the principles and advantages of Traveling-wave tubes (TWT) and klystrons achieving high power and bandwidth [11].

Solid state electronics sources

- **Gunn diodes:** gunn diodes are semiconductor devices made of three N-doped regions. The regions on the terminals are highly doped while other thin lightly N-doped region lies in between. Because of this characteristic structure, Gunn diodes present negative resistance above a certain voltage. This property allows the usage of these devices as oscillators. Gunn oscillators can operate in all of the terahertz band, but the most common are known to to operate near 100 GHz. Those are mostly used to be frequency multiplied.
- **Frequency multipliers:** semiconductor based frequency multipliers can generate terahertz radiation by means of distorting sub-terahertz signals with non-linear devices and then selecting one of the harmonics produced with appropriate filters.

Lasers

- **Quantum cascade lasers:** the active region of these lasers is a repetition of thin semiconductor layers, forming a superlattice of quantum wells. Here, a single electron injected into the conduction band will emit a series of photons when cascading through

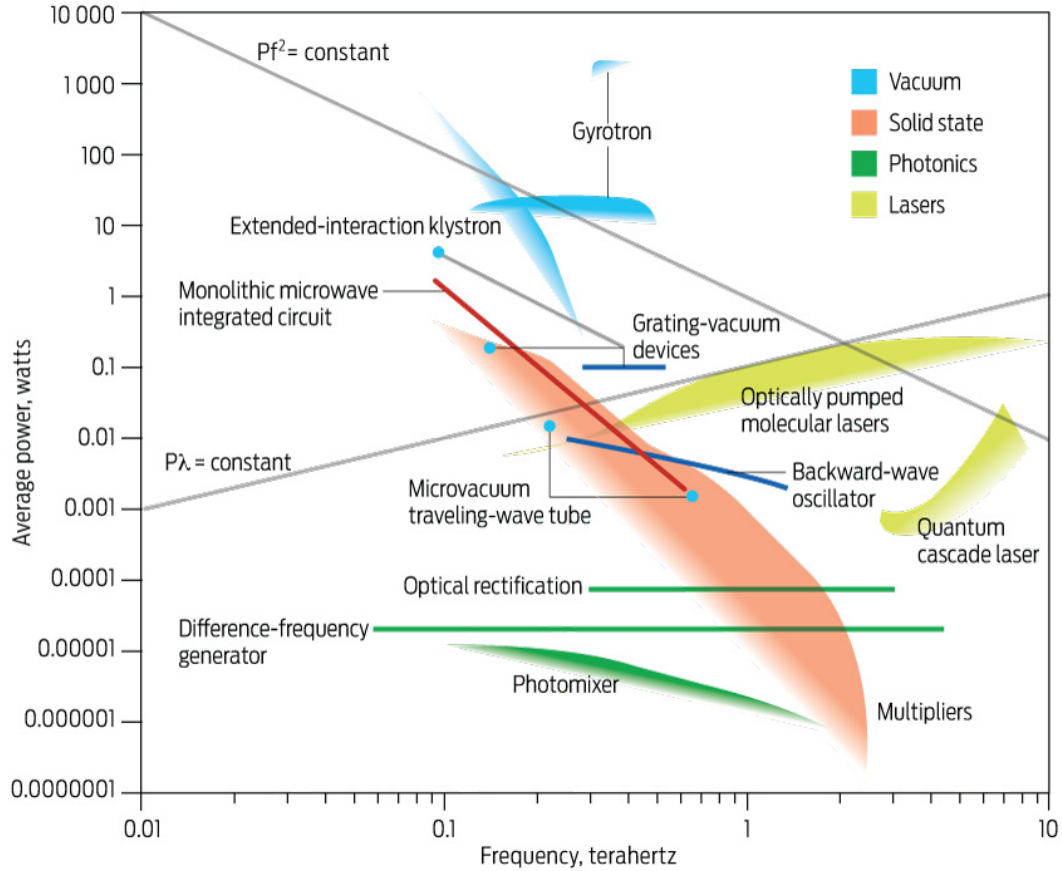


Figure 2.3: Comparison between various THz sources. Source: [9]

intersubband transitions. Quantum cascade lasers (QCLs) can operate in the mid and far-infrared regions. They can operate as radiation sources in the terahertz region with tens of mW when cooled [12].

- **Optically pumped molecular lasers:** lasers in which the active medium is a molecular gas that is pumped with an optical source, typically a gas lamp or diode lasers. They radiate in the THz band due to rotational and vibrational transitions.

Photonic sources

- **Pulsed lasers:** femtosecond lasers (usually Ti:sapphire lasers) are used to produce very short pulses of laser radiation. These pulses are used to generate terahertz radiation by using the photo-Dember effect, optical rectification or a photoconductive antenna [13]. Time-domain terahertz spectroscopy is performed with this type of radiation source [3].
- **Difference-frequency generator and sum-frequency generator:** non-linear crystals have been used to generate THz and sub-THz radiation by combining two high intensity beams. In the non-linear medium the photons of the incoming beams can interact to form new photons with a frequency equal to the frequency difference or sum of the two pump beams.

- Photomixers:** a photomixer is a compact semiconductor device used to generate CW THz radiation. These devices are typically constructed by placing a metallic antenna on a photoconductive semiconductor substrate, usually LT-GaAs. A lens is attached to the back of the substrate to collimate the output radiation [5]. The terahertz waves are produced when two laser beams with different frequencies are focused on the device and generate an intensity beat at the difference frequency. The incoming light will produce the generation of carriers in the semiconductor. An external voltage needs to be applied to move the carriers, producing a current which is coupled into an antenna. As the amount of carriers in the semiconductor is proportional to the intensity of the incident light, the beat between the two laser will modulate the current in the antenna. When the frequency difference of the two lasers is appropriately tuned, terahertz radiation is produced. A typical photomixer scheme can be seen in Figure 2.4.

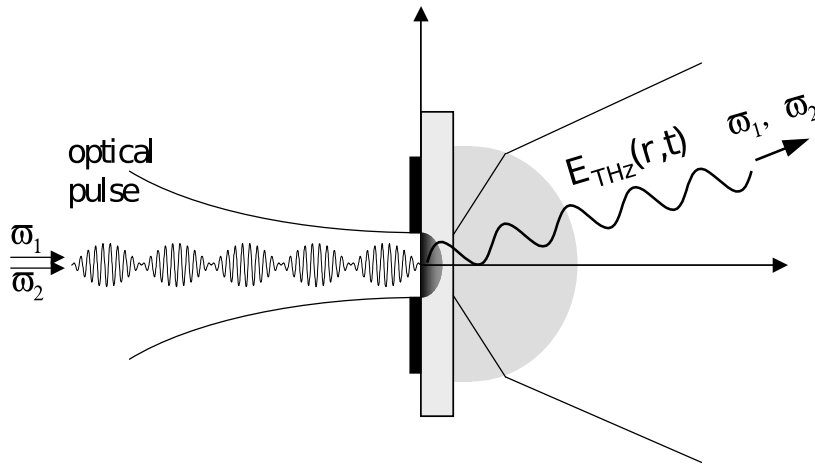


Figure 2.4: Photomixing process. From the left, two laser sources with frequencies ω_1 and ω_2 illuminate a photomixer. This produces the output THz radiation on right E_{THz} [5].

Photomixers are potentially ultra-broadband, being able to achieve scanning ranges from 60 GHz to 1.8 THz [14]. They can be easily modulated [15] and can perform with low noise and high spectral resolution [16] if a high-quality dual-frequency laser system is available [5]. These qualities makes them specially suitable for broadband and precise spectroscopy, telecommunications and imaging. The main drawback of these devices is the low power output, typically in the range of microwatts [5, 16]. One of the reasons for this limitation is the low thermal power dissipation of the substrate that limits the applicable input power, while the output power depends on the square root of the input power.

2.2. Lasers

Lasers are devices that produce temporally and spatially coherent light. This means that the output radiation has a narrow spectral width, high phase stability and its wavefront is relatively plane (collimated). The name comes from the acronym *Light Amplification by*

Stimulated Emission of Radiation. The quantum process of stimulated emission on which laser are based on was first proposed by Einstein in 1917. But it was not until 1960 that the first lasers appeared. Today they are applied in many fields: high speed telecommunications, measurement devices, laser surgery, storing and reading information in optical disk drives, engraving, metal cleaning, among many others.

The characteristic coherence that lasers exhibit is a consequence of the phenomenon that they use to generate light: stimulated emission. This phenomenon is going to be explained in the next paragraphs.

Quantum mechanical systems like atoms, molecules or subatomic particles, have discrete allowed energy states. For example, electrons in atoms can orbit the nucleus only in certain energy states, where the electron's wave function is stationary. The distribution of electrons in these states determines the atom's wave function. On the other hand, molecules have very complex energy states influenced by its electronic configuration and the bonding between its atoms.

Since the energy of the system has to remain constant when an atom or a molecule transits from one energy state to another, the atom or molecule has to absorb or radiate energy to the medium. The most common way to exchange energy is by the emission or absorption of photons. The photon emitted or absorbed in a transition must have equal energy than the difference between the two states. Since the energy of a photon is strictly related to its wavelength, transitions between specific energy states radiate and absorb photons with fixed wavelengths. This relation is shown in equation (2.1).

$$\Delta E_{\text{energy states}} = h\nu = h\frac{c}{\lambda} \quad (2.1)$$

where $\Delta E_{\text{energy states}}$ is the difference between the two energy levels of the transition, h is Planck's constant and ν is the photon's frequency which is equal to the velocity of light c divided by its wavelength λ . There are three different possible processes that can occur when a transition takes place:

- **Absorption:** the energy of the photon is taken by the atom or molecule, transitioning to a more energetic (excited) state.
- **Spontaneous emission:** an excited system drops to a lower energy level, releasing a photon.
- **Stimulated emission:** a photon can interact with a excited state, inducing the decay of the system into a lower state in a way such that another photon of the exactly same wavelength, phase and direction of the passing photon is emitted.

This processes are represented in Figure 2.5. For a scenario consisting in a group of atoms with two energy levels with a incident flow of radiation, the average rates of absorption, spontaneous emission and stimulated emission can be calculated by:

$$\left. \frac{\partial N_2}{\partial t} \right|_{\text{spontaneous emission}} = - \left. \frac{\partial N_1}{\partial t} \right|_{\text{spontaneous emission}} = -A_{21}N_2 \quad (2.2)$$

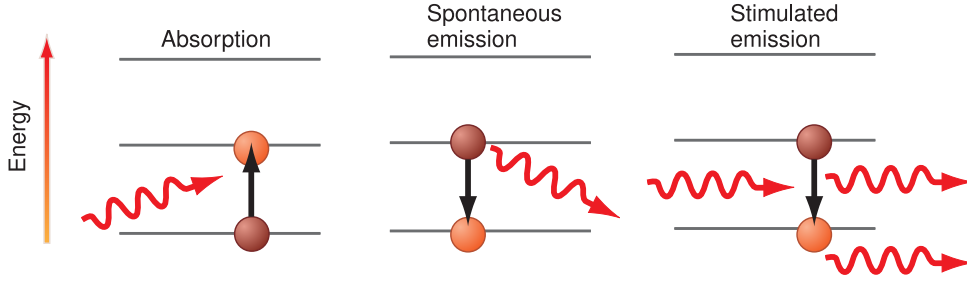


Figure 2.5: The three basic processes by which photon-assisted transitions occur. Orange- and red-filled circles indicate final and initial levels, respectively [17].

$$\left. \frac{\partial N_2}{\partial t} \right|_{\text{stimulated emission}} = - \left. \frac{\partial N_1}{\partial t} \right|_{\text{stimulated emission}} = -B_{21} \rho(\nu) N_2 \quad (2.3)$$

$$\left. \frac{\partial N_1}{\partial t} \right|_{\text{absorption}} = -B_{12} N_1 \rho(\nu) \quad (2.4)$$

Where N_2 is the number of atoms in the higher or excited state and N_1 is the number of atoms in the lower or ground state, A_{21} , B_{21} are coefficients for this particular transition know as the *Einstein coefficients*, and $\rho(\nu)$ is the density of photons with frequency ν . The B coefficients are related as follows:

$$\frac{B_{21}}{B_{12}} = \frac{g_1}{g_2} \quad (2.5)$$

where g_i is the degeneracy of state i ¹.

It can be seen that absorption and stimulated emission are proportional to the radiation density, and that absorption is only dependent on the amount of atoms in the lower energy level, while stimulated emission is only dependent on the number of atoms in the upper level. Given that there are no degenerate states, the total or net transition to the lower state is:

$$\left. \frac{\partial N_1}{\partial t} \right|_{\text{net}} = \left. \frac{\partial N_1}{\partial t} \right|_{\text{stimulated}} - \left. \frac{\partial N_1}{\partial t} \right|_{\text{absorption}} + \left. \frac{\partial N_1}{\partial t} \right|_{\text{spontaneous}} = B_{21}(N_2 - N_1)\rho(\nu) + A_{21}N_2 \quad (2.6)$$

In regular conditions, i.e. thermal equilibrium, it is expected that a population of particles with various possible states follows the Boltzmann distribution:

$$F(\text{state}) \propto e^{-\frac{E}{kT}} \quad (2.7)$$

¹Degeneracy or multiplicity of a energy level is the amount of quantum states that share that energy level.

where E is the energy of the state, k is Boltzmann's constant and T is the thermodynamic temperature. For any pair of energy levels of values $E_2 > E_1$, the relative population of the more energetic level to the lower is given by:

$$\frac{N_2}{N_1} = e^{-\frac{E_2 - E_1}{kT}} \quad (2.8)$$

If the expressions of equation (2.6) is positive, it means that more electrons are dropping and therefore there is a positive amount of energy being radiated. But since the photons emitted in the process of spontaneous emission are not necessarily in the same direction or in phase with the incoming radiation, it is necessary that $(N_2 - N_1)$ is positive to have coherent amplification of the incoming radiation. As it can be seen in (2.8), in regular conditions the lower energy levels are more populated than the higher ones and, therefore, there can be no amplification. To use a medium to amplify it is required to force a higher population in the upper level ($N_2 > N_1$), a condition that is called *population inversion*. This is the principle behind laser amplification.

Since $\partial N_2 / \partial t < 0$ the population N_2 will decrease until $\partial N_2 / \partial t = 0$. To maintain the population inversion an external mechanism is required to drive the atoms in the medium from the ground state to the upper state. This process is called *pumping*. The energy applied to excite the atoms can be in the form of electricity, heat, or even with electromagnetic radiation, depending on the nature of the medium. Typical laser media are molecular gases (CO_2 , $HeNe$), noble gases, semiconductors and doped fibers. In more realistic systems, the pumping mechanism utilizes more than two energy levels to maintain the population inversion, as seen in [?].

A laser is, in a simplified manner, an amplifier with a positive feedback loop. The amplified radiation is fed back into the lasing medium, where it will be amplified even more, until the pumping process is not fast enough to continue the amplification and a steady state point of operation is reached. The initial radiation or seed can be an external signal or, most commonly, the spontaneous emission from the active medium. The feedback loop can be constructed with free beam optics (mirrors, gratings, etc) or fibers, forming an optical resonating cavity. Only radiation that fits one of the optical modes from the cavity can form standing waves and be constantly amplified in the medium, meaning that the feedback loop itself is also a very narrow filter. Part of the circulating radiation exits the cavity through a partially transparent mirror, forming the laser light. This is usually achieved by designing one of the mirror with a small transmittance, usually in the range of 1 % - 30 %, depending on the gain of the laser medium.

In synthesis, the main components of a laser (as seen in figure [?]) are:

- **Lasing or gain medium:** collection of atoms or molecules that radiate at the desired wavelength with the process of stimulated emission.
- **Pumping or excitation mechanism:** the mechanism used to produce and maintain the population inversion on the gain medium.
- **Optical cavity:** the resonant cavity where the radiation is contained to increment the density of photons with the desired frequency and therefore increase the rate of

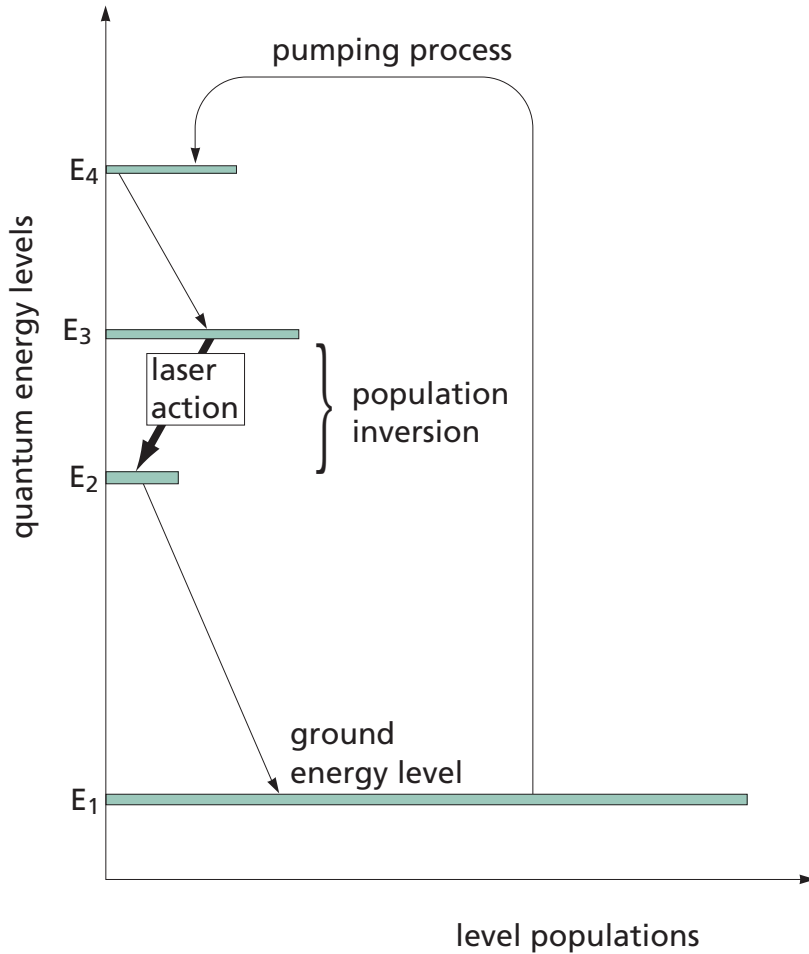


Figure 2.6: A four-level laser pumping system [18].

stimulated emission.

Lasers come in a variety of wavelengths and powers, some emit only at a fixed wavelength while other can be tuned over a range. Stability, power, tunability and size are some of the main characteristics that are relevant for selecting a laser for each specific application. There are continuous-wave (CW) and pulsed lasers. Two laser types will be reviewed since they are of special interest for this work: diode lasers and fiber laser.

2.2.1. Diode lasers

Diode lasers are semiconductor lasers that use a highly doped p-n junction as the active medium. The photons are generated by the recombination of carriers and holes in the junction. The bandgap of the semiconductor material determines the wavelength of the radiated light. Commercially available wavelengths go from 380 to 1650nm [19] and the typically used semiconductor materials are GaAs, AlGaAs, InGaP, GaInNAs, InP, GaInP [20]. The most common pumping method used in this kind of laser is a direct current over the junction, but other methods like optical pumping are also possible [20].

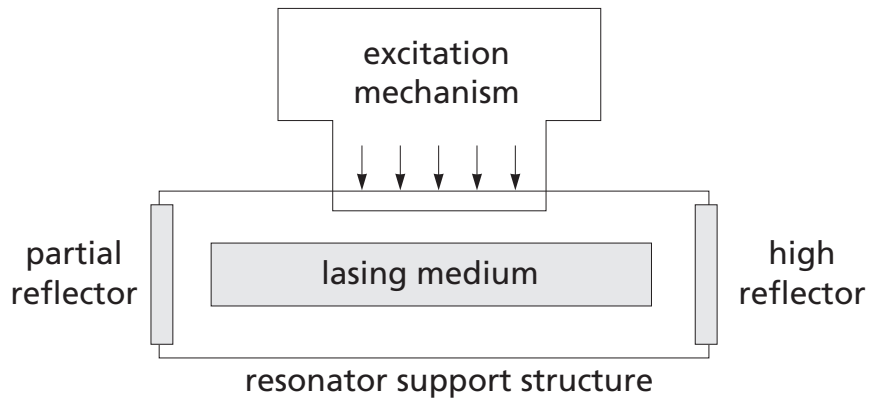


Figure 2.7: Schematic diagram of a basic laser [18].

Sometimes, diode lasers are called laser diodes (LDs) but it is convenient to make a differentiation: diode lasers are laser devices that consist of laser diodes integrated into external cavities including beam collimation optics [19]. One surface of the semiconductor crystal is then used as a reflective surface by cleaving the material along its crystal planes [12] thanks to the refractive index difference between the semiconductor and the surrounding air, making the gain medium work also as an optical resonator. The other surface needs to be anti-reflection coated to match to the external cavity.

Diode lasers are a very common type of laser because they have very interesting advantages: high power, high efficiency, small size, and they can be easily modulated with electronics by controlling the electric current injection [12]. Depending on the application, different configurations can be used: from high-power stacked diode bars that radiate hundreds of watts with poor beam quality to low power small arrangements emitting in a single mode [19].

The linewidth of diode lasers is usually in the range of hundreds or tens of megahertz, but can be improved by using external cavity, typically up to the kilohertz range. The temperature of the junction affects the bandgap and therefore modifies the wavelength. This means that the temperature has to be controlled but also means that the wavelength can be tuned by adjusting the operating temperature. Tuning can also be performed by modifying the resonator length or adjusting intercavity filters (like rotating the diffraction grating) in external cavity lasers [19].

The electrical-to-optical power conversion efficiency is typically around 50 %, but depends on many factors like the wavelength or output power [19]. The output beam of laser diodes can be asymmetric, astigmatic and with large divergence due to the small thickness of the active layer in the semiconductor crystal [21]. This may require additional optics for collimation and coupling, which reduces the efficiency. Worst beam characteristics are more common in high power devices.

2.2.2. Fiber lasers

Fiber lasers are those in which the active medium is an optical fiber. This is achieved by doping the glass fiber with rare-earth metal ions like Nd, Yb, Er, Tm and Ho [12]. Rare-earth atoms are then pumped optically by laser diodes coupled into the same fiber. Laser diodes can deliver high power and are commonly used in industrial machinery like laser cutters, but can also perform very well in high precision applications working with great stability and high coherence.

The fibers used as gain medium are mostly made of glass because plastic fibers are hard to dope and have higher absorption. The composition of the glass is very relevant as certain materials have high absorption in certain wavelengths. Also, the amount of dopant that can be applied depends on the host glass [22]. Table 2.1 show the most commonly used materials.

Ion	Host Glass	Emission wavelength
neodymium (Nd ³⁺)	silicate and phosphate	0.9-0.95 μm ; 1.01-1.03 μm ; 1.32-1.35 μm
ytterbium (Yb ³⁺)	silicate	0.98 - 1.1 μm
erbium (Er ³⁺)	silicate, phosphate and fluoride	0.55 μm ; 1.5-1.6 μm ; 2.7 μm ; 3 μm
thulium (Tm ³⁺)	silicate, germanate and fluoride	0.48 μm ; 0.8 μm ; 1.45-1.53 μm ; 1.7-2.1 μm
praseodymium (Pr ³⁺)	silicate and fluoride	0.49 μm ; 0.52 μm ; 0.6 μm ; 0.635 μm ; 1.3 μm
holmium (Ho ³⁺)	silicate and fluoro-zirconate	2.1 μm ; 2.8-2.9 μm

Table 2.1: Most common laser active ions, typical host glasses and operating wavelengths [22].

Different dopants require different pump wavelength, since the photon energy must match with the energy difference between the levels of the metal ions used to achieve population inversion. The wavelength of the pump light can be longer or shorter (upconversion) than the wavelength of the emitted light [22].

The light in the gain medium needs to be confined in a optical resonator. For this purpose, reflectors on the end of the fiber or fiber loops are used. In the case of reflectors, dielectric mirrors or dielectric coating can be placed at the end face of the fiber but the most robust designs use fiber *Bragg gratings*². On the other hand, loop filters are made by using fiber couplers and passive fiber.

2.3. Laser injection locking

Injection locking is the effect produced by injecting a signal from one oscillator, known as master, into another oscillator, named slave. Even small signals injected to the slave oscillator can influence dramatically its behavior when the signal injected is close enough to the free-running frequency of the slave [23], *locking* its frequency to the master's.

This effect was probably first observed by Christiaan Huygens, when he noticed that two

²Bragg grating are periodic or aperiodic perturbation of the refractive index in the core of an optical fiber that produce reflections of only a narrow band of the incoming light.

wall clocks synchronized when placed close enough, but became free-running when placed further apart [24]. Electrical oscillators and lasers can also be locked through this mechanism.

Injection locking of lasers is very useful since it allows to improve the dynamics of powerful lasers [23], reducing laser noise [25] and optical linewidth [25] when a more stable lasers is used as a master. A suitable coupling mechanism between the lasers should match the modes of the injected signal to those of the cavity of the slave laser. To study the injection locking process, it is useful to model a laser as a regenerative amplifier with an external signal injected. In this case, a ring laser is used following the formulation by Siegman [24], but the results can be generalized. The power amplification $|\tilde{g}(\omega)|$ from input to output for an injected signal with frequency (ω) close to the radiating frequency of the laser (ω_0) can be approximated using the expression: [24]

$$|\tilde{g}(\omega)| \approx \frac{\gamma_e^2}{(\omega - \omega_0)^2} \quad (2.9)$$

where γ_e is the energy decay rate of the laser cavity due to external coupling. It can be related to the external coupling through an output mirror of reflectivity R with (2.10) if $R \approx 1$.

$$R = \exp(-\gamma_e T) \approx 1 - \gamma_e T \quad (2.10)$$

Where T is the transit time for one round trip inside the cavity. The external decay rate γ_e and the external cavity Q_e are given by:

$$\gamma_e = \frac{\omega}{Q_e} \approx \frac{1 - R}{T} \quad (2.11)$$

It can be seen from equation (2.9) that the gain would go to infinity if $\omega \rightarrow \omega_0$. This is, in reality limited by the maximum gain of the media.

The injected signal can be amplified independently from the free-running oscillation of the laser given that they are not too close. Beating and interference effects could happen otherwise.

If the injected signal has a fixed intensity of I_1 , the amplified output intensity would be $|\tilde{g}(\omega_1)|^2 I_1$. This magnitude will increase as ω_1 gets closer to ω_0 . Since the gain of the laser media is limited, the injected signal will begin to steal gain from the laser medium until the gain of the free-running oscillation I_0 is suppressed. At this point, the amplitude of the injected signal will no longer increase as there is no more energy available in the cavity. Therefore, the injection locking range can be calculated, for small coupling, solving (2.12).

$$|\tilde{g}(\omega_1)|^2 I_1 = \frac{\gamma_e^2}{(\omega_1 - \omega_0)^2} I_1 \approx I_0 \quad (2.12)$$

Then, the injected signal will overtake the free-running oscillation near the points given by:

$$|\omega_1 - \omega_0| \approx \gamma_e \frac{E_1}{E_0} \approx \frac{\omega_0}{Q_e} \sqrt{\frac{I_1}{I_0}} \quad (2.13)$$

Thus, the injection locking range is:

$$\Delta\omega_{lock} \approx 2\gamma_e \frac{E_1}{E_0} \approx \frac{2\omega_0}{Q_e} \sqrt{\frac{I_1}{I_0}} \quad (2.14)$$

This result is valid for $I_1 \ll I_o$ and it is applicable to any other kind of injection-locked oscillator, like electronic or mechanical. The behavior of the laser as a function of the injected signal's frequency is depicted in Figure 2.8.

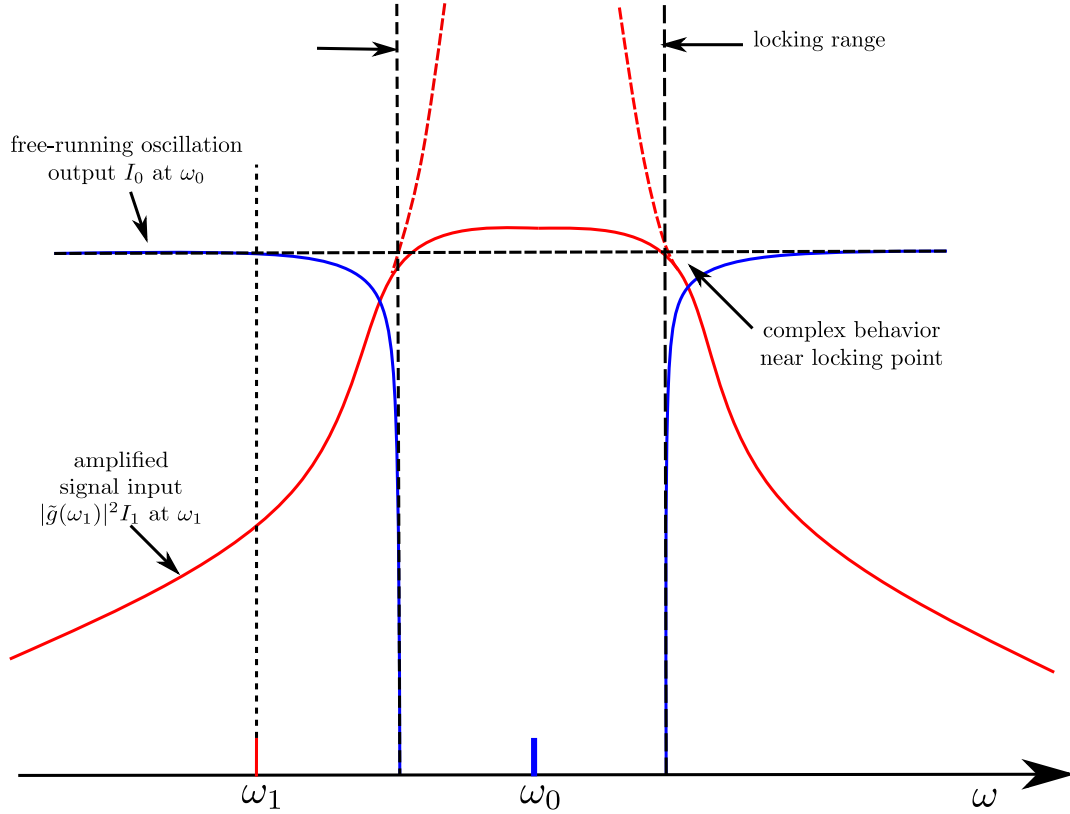


Figure 2.8: Output of the laser as the injected signal becomes closer to the free-running oscillation [24].

The phase angle $\phi(\omega_1)$ of the output signal with respect to the injected signal varies within the tuning range (see Figure 2.9) can be calculated by: [24]

$$\phi(\omega_1) = \sin^{-1} \left(\frac{\omega_0 - \omega_1}{\Delta\omega_{lock}} \right) \quad (2.15)$$

2.4. Spectroscopy

Spectroscopy is the study of the interactions between light and matter [4]. This interaction depends on the composition and state of matter, and therefore, it allows the observation of the fundamental properties of matter through the observation of the wavelengths of light absorbed and emitted. [26]

The history of spectroscopy can be traced back to 1814 when Joseph von Fraunhofer diffracted a beam of sunlight using one of his high-quality prisms. He observed that, besides the expected colors of the rainbow, a pattern of dark lines of unknown origin was present.

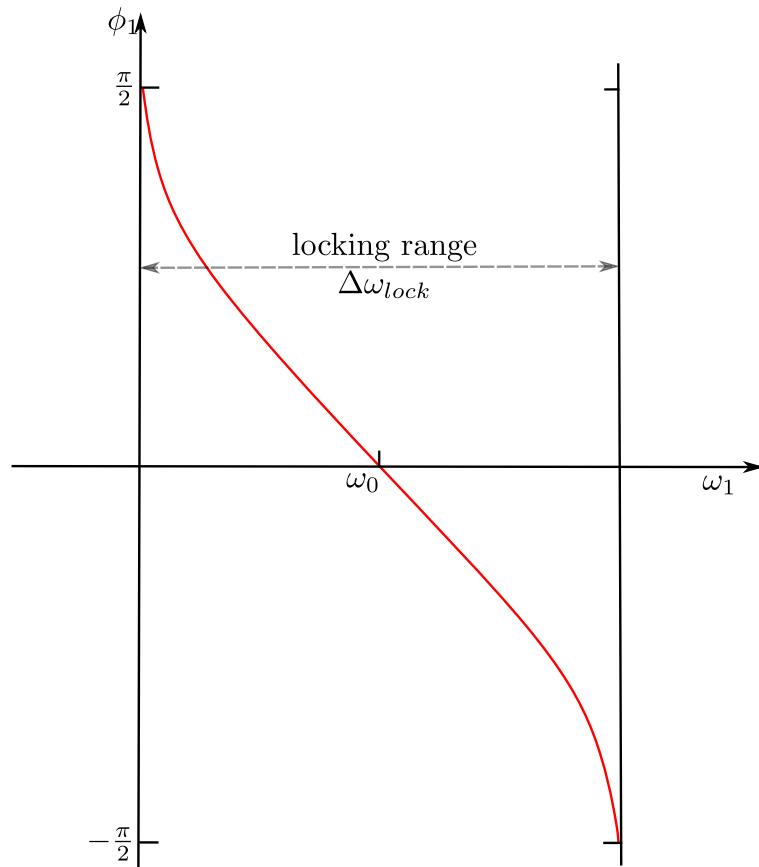


Figure 2.9: Relative phase angle of the two signals versus frequency within the injection locking range. [24]

He then performed the same experiment but with another star, Betelgeuse, and found that the pattern was different. He arrived to the conclusion that these lines were related to the composition of the object he was observing [27]. Some decades later, Gustav Kirchhoff and Robert Bunsen found the correspondence of some of the lines observed by Fraunhofer to the ones present in the light produced when metals were burnt in flames, demonstrating that some of the sunlight's lines were a direct consequence of the atomic composition of the Sun [27].

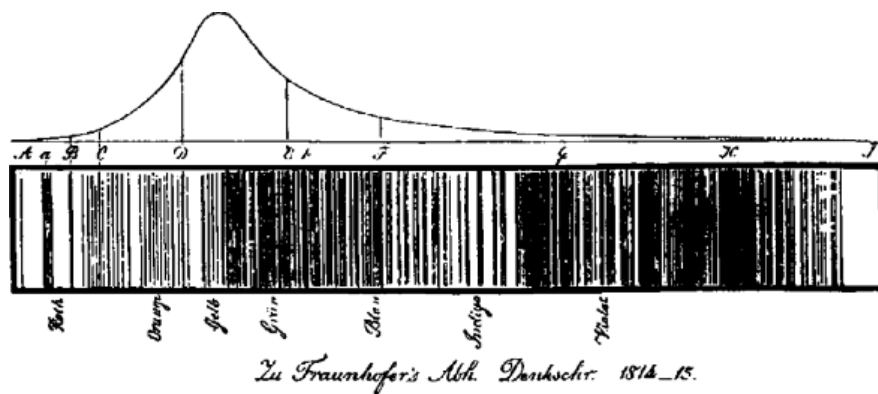


Figure 2.10: Spectral lines observed by Fraunhofer. [27]

Today, spectroscopy is used to study a wide variety of physical phenomena, from electrical atomic transitions to biological systems' dynamics [5] and has important applications in many fields like astronomy, chemistry, biology and medicine.

Each atomic element or molecule has a characteristic set of quantum energy states and, therefore, it has a characteristic set of possible transitions between these states. As it was explained in Section 2.2, each transition is strictly linked with the emission or absorption of radiation with a specific wavelength, meaning that each element can only absorb or emit light in specific group of wavelengths, called spectrum. In spectroscopy, these spectra are used as fingerprints that allow the detection of elements.

Atoms have their energy levels dictated by the probability distribution of electrons around their nuclei. Atomic states are formed by the quantization of motion, orbital and spin angular momenta of all electrons [26]. Molecules have their energy levels determined in part by the potential energies associated with the interatomic forces binding the atoms. The type of the bond (ionic, covalent) plays a role in determining the energy-level structure of the molecule [12]. The three main transitions that molecules experience are:

- **Rotational transition:** Changes in the rotational momentum produce mostly microwave and far-infrared radiation;
- **Vibrational transitions:** Bonds between atoms can be quantum-mechanical harmonic oscillators (similar to microscopic masses joined by a spring) with different vibrational modes. Transitions between them radiate mostly in the infrared portion of the spectrum;
- **Electrical transitions:** Transitions in the energy states of the electrons produce radiation mostly in the visible and ultraviolet.

These transition are not necessarily independent, as there can be transition between two types simultaneously, like vibronic transition where the electrical and vibrational state are changed in conjunction.

In astronomy, spectroscopy is one of the main sources of information [27]. By comparing the spectra from astronomical observation with the known spectra of atoms and molecules, astronomers can obtain information about: [27]

- The composition of the observed object is inferred by knowing which atoms or molecules produce the observed transitions.
- The temperature can be determined by identifying which of the component's transitions are taking place, thus a degree of excitation of the system is predicted.
- The abundance of the species if the intrinsic strength of the transitions is known.
- The motion of the species relative to the Earth produces a shift in the wavelength of the species, known as the Doppler shift. This is proportional to the relative movement and to the distance, allowing a dynamic mapping of the cosmos.
- Magnetic fields can be indirectly observed, because they produce a split between energy levels which possess angular momentum.

To determinate the spectra of elements, it is necessary to solve the appropriate quantum mechanical models. For complex atoms, with a high number of electrons and protons, solving

these equations is not trivial. Numerical solutions can be calculated with modern computers [26], but laboratory data is still used as a reliable reference. [27].

In astronomical spectroscopy, it is possible to observe both emission spectra and absorption spectra. In the first case, atoms or molecules under excitation will have constant transition between energy levels that will irradiate [27]. Even gas phase molecules in low density and low temperature clouds will have transitions, mostly at lower energy levels. For example, HI or 21 cm line is produced by a transition in neutral atomic hydrogen [27] that is used in astronomy to map galaxies.

Absorption lines can be observed when a known source's radiation passes through the interstellar medium [27]. A typical situation where absorption spectra is observed is at the atmosphere of stars. The core of the star provides a continuum light source following the black body radiation curve with the temperature of the star. Species in the photosphere of the star are observed as in absorption against this curve [27]. This is the nature of spectroscopic observations that led to the discovery of the helium (He) element.

2.4.1. Terahertz spectroscopy

Terahertz spectroscopy is specially appealing for the number of molecular transitions in this band. Many molecular species have very narrow and unique spectral lines in this region which is helpful to detect and identify chemicals. [5] Many transitions between quantized rotational states can be traced to absorption lines in the THz and microwave regions. This is why terahertz spectroscopy is particularly suitable for detection of molecules in gaseous form, for example, in atmospheric monitoring or studying the composition of the interstellar medium [5]. With high-resolution spectroscopy, it is possible to determinate molecular structures and study molecular collisions by resolving in detail the shape of the absorption lines [5].

Vibrational states are originated by the periodic motion, angular or longitudinal, of the constituent atoms of the molecule. The number of vibrational modes is proportional to the number of atoms. For linear molecules, the number of vibrational modes is $3N - 5$. For nonlinear molecules, it is $3N - 6$.

Vibrational transitions are specially important for the study of macromolecules. Molecular structure of biological and chemical molecules can be determined with great detail through the study of intermolecular and intramolecular vibrations. For example, the crystalline state of drugs can be investigated using THz spectroscopy [3]. This can be used to monitor the manufacturing process of pharmaceutical products in a non-destructive form.

Other important application of terahertz spectroscopy is the detection of concealed explosives. Common energetic explosives are characterized by their strong and unique absorption lines [5]. Proteins and other biological molecules are also good candidates for THz detection.

Chapter 3

Design and Implementation

The proposed design for the terahertz synthesizer consists in a UTC-photomixer fed by two infrared laser signals, one of which is tunable over a wide range in discrete steps (coarse tuning) while the other can be continuously tuned in a small range of at least the distance between steps of the coarse tuned signal (fine tuning). This allows the synthesis of all the frequencies in a wide range. The system is connected through fiber optics, and it is represented in a simplified form in Figure 3.1.

As it was explained in 2.1.1, the frequency of the generated terahertz radiation ν_{THz} is equal to the difference of the two signals coupled into the photomixer:

$$\nu_{IR1} - \nu_{IR2} = \nu_{THz} \quad (3.1)$$

The two infrared signal (ν_{IR1} and ν_{IR2}) are generated from a low noise, highly coherent, single frequency Koheras AdjustiK E15 fiber laser (master laser or ML from now on). The laser signal is split in two and used as a common reference.

The continuously modulated (ν_{IR2}) signal is generated by modulating the master laser's amplitude with a variable frequency ν_{mod} and selecting the lower side band (LSB), filtering out the carrier and upper side band (USB). For the stepped signal (ν_{IR1}) we modulate the master laser with an optical comb generator using a fixed frequency ν_{comb} and then lock a tunable diode laser (slave laser) to one of the comb lines by injection locking. The mechanisms used to produce each of these signals are explained in detail in the following sections (3.1, 3.2). Therefore, the frequency of the signals can be expressed as:

$$\underbrace{(\nu_{ML} + n \times \nu_{comb})}_{\nu_{IR1}} - \underbrace{(\nu_{ML} - \nu_{mod})}_{\nu_{IR2}} = \nu_{THz} \quad (3.2)$$

where n is an integer, corresponding to the n^{th} -comb line . Then,

$$n \times \nu_{comb} + \nu_{mod} = \nu_{THz} \quad (3.3)$$

By choosing $\nu_{comb} = 10$ GHz and with ν_{mod} ranging from 9 to 20 GHz we can synthesize any frequency in a range limited only by the comb lines available for injection locking. For example, frequencies up to 100 GHz can be synthesized if the slave laser can be locked to the 9th ($n = 9$) upper comb line.

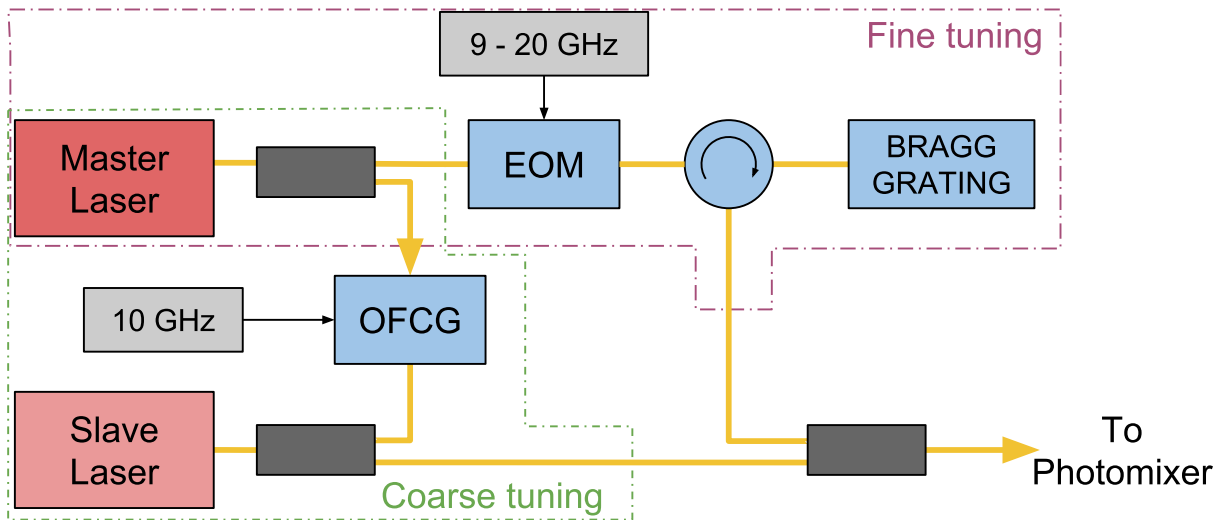


Figure 3.1: Simplified block diagram of the dual frequency synthesizer. It is divided in two subgroups: the coarse or discrete tunable signal and the fine or continuously tunable signal. The first subgroup, delimited by the green dashed line, is based on the optical comb generator (OFCG) and the second, delimited by the magenta line, is based on the electro-optical modulator (EOM). Yellow connectors represent optical fibers and black electrical connections.

3.1. Wide range, discrete tunable signal

To generate an infrared signal with a terahertz tuning range and good stability, a Velocity 6329 tunable diode laser (slave laser) is injection-locked to one of the lines of an optical frequency comb generator (OFCG). The slave laser will then oscillate at virtually the exact frequency of the comb line, and as the comb lines inherit the optical stability from its input, the slave laser will be oscillating with the stability of the master laser used as the input of the OFCG. Since the slave laser has a range from 1496 to 1583 nm, approximately 200 THz, the range of this setup is determined by the number of comb lines with enough power to lock the slave laser.

The locking process is achieved by injecting the output of the comb generator into the laser and then tuning the laser's cavity until its resonance frequency is close enough to the selected comb line, so that the laser is locked by the comb line. To allow the injection of the comb signal into the laser cavity, the fiber-coupling of the slave laser had to be changed since the original coupling mechanism has attached an optical isolator.

A manual fiber polarization controller is placed at the input of the OFCG to match the master laser's polarization to that of the OFCG cavity and another is placed at its output to improve the coupling into the slave laser. Figure 3.2 shows the conceived design.

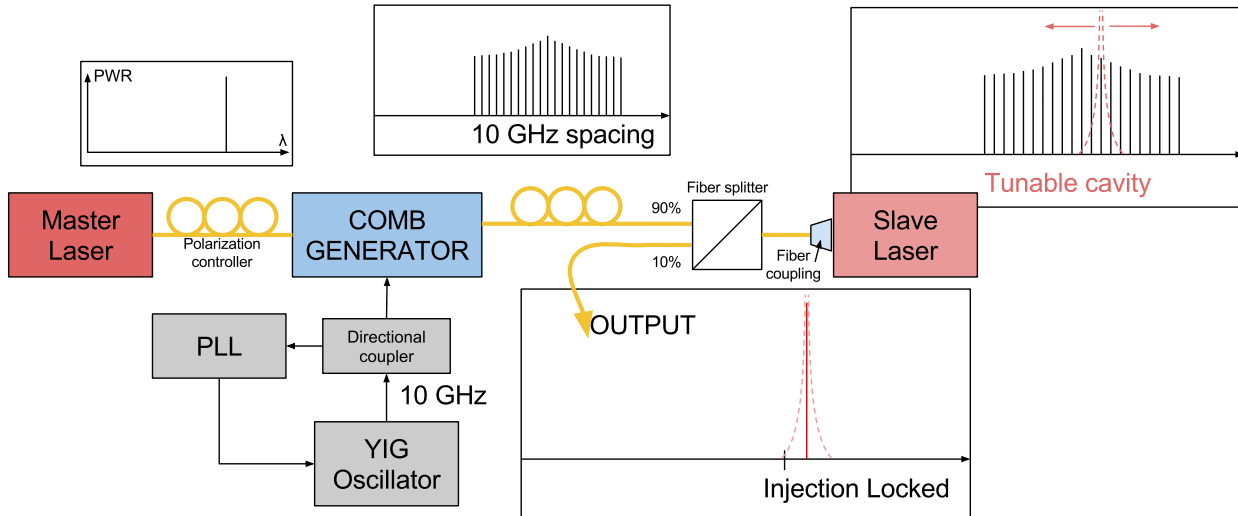


Figure 3.2: Block diagram of the system designed to produce a stable, discrete tunable infrared signal. A highly stable laser (Master Laser) is used to generate a set of discrete signal with an optical comb generator. This lines are injected to a slave laser which is locked to one of the comb lines by tuning its cavity. Optical fiber paths are in yellow while electrical signals are in gray.

3.1.1. Optical frequency comb generator

The optical comb generator modulates the master laser, producing periodic pulses with a repetition rate equal to the period of the RF reference signal. In the frequency spectrum, this is equivalent to a series of lines equally spaced with a frequency spacing equal to the RF reference. To achieve high stability, a YIG oscillator is used as RF reference. A DC bias voltage is added to the RF signal to improve the efficiency by centering the modulation at the half-wave voltage (V_{π}).

YIG oscillator

The YIG oscillator used in this application is a MLPF-1500FM from Micro Lambda Wireless. It has a fixed free-running frequency of 10 GHz and a FM driver that allows a deviation of ± 56 MHz [28].

To stabilize the oscillator, a digital PLL control system is implemented. It is based on a control system created at the Millimeter-waves Laboratory from Cerro Calán Observatory [29].

The core of the control loop is the AD9901 digital phase/frequency discriminator. It is capable of directly comparing phase/frequency inputs up to 200 MHz, without indeterminate phase detection zones [30]. This means that the frequency of the oscillator must be reduced to fit within this range and also that the sinusoidal waveform must be translated to a digital signal.

A sample of the YIG oscillator's output is taken with a directional coupler. The frequency is then reduced using a HMC362S8 divide-by-4 static divider and mixed with a 2.4375 GHz signal generated by a Valon 5007 dual synthesizer. Some stages of attenuation and filtering are used to match power ratings and eliminate harmonics. The signal that is introduced to the PLL board has a power of -30 dBm and a frequency of:

$$f_{\text{sample}} = \frac{f_{\text{YIG}} + f_{\text{phase noise}} + f_{\text{offset}}}{4} - f_{\text{LO}} \quad (3.4)$$

where f_{YIG} is the nominal frequency of the YIG oscillator (10 GHz), $f_{\text{phase noise}}$ is the phase noise (assumed additive), f_{offset} is the difference between free-running and nominal frequency, f_{LO} is the local oscillator's frequency for the mixing process (2.3475 GHz).

$$f_{\text{sample}} = \frac{f_{\text{phase noise}} + f_{\text{offset}}}{4} + 62.5 \text{ MHz} \quad (3.5)$$

The 62.5 MHz reference is the result of a 2.0 GHz signal divided by 32 using a Valon 3008 frequency divider module. To eliminate the harmonics, a 45 MHz low pass filter is used.

Inside the PLL board, each sinusoidal signal is amplified and then converted to a digital Transistor-Transistor Logic (TTL) signal. Afterwards, the phase/frequency discriminator compares both signals and delivers a square signal with a duty cycle proportional to the frequency difference between the oscillator and reference inputs. A differential amplifier levels the signal which is then converted to a DC voltage by a second-order active filter with a variable gain, which is controlled manually with a potentiometer. The DC voltage has a range of $\pm 10\text{V}$ which is then transformed to a $\pm 100\text{mA}$ current signal that drives the FM coils in the YIG oscillator, changing its frequency. The gain of the control loop has to be such that a $\pm 56 \text{ MHz}$ deviation is translated to a $\mp 100 \text{ mA}$ signal in the driver. A simplified diagram of the complete PLL system is shown in Figure 3.3.

The YIG oscillator and the control system are going to be integrated into a single standalone device, to facilitate the handling and improve its operation. Basically, this consists in the encasing of the electronics and implementation of a dedicated power supply.

The casing of the YIG and its control loop will protect these devices against electromagnetic noise, dust and any other external particles that could harm the electronics. With the inclusion of a dedicated power supply there will be no need for external power supplies, facilitating the use of the device and freeing lab equipment. For the case a 1U metal rack was selected. For the power supply, the requirements shown in Table 3.1 must be met.

These requirements were elaborated considering the maximum current drawn by each device according to its corresponding datasheet. For the PLL board an estimation was used since there is no data regarding the maximum power consumption of the overall board.

To satisfy these specifications, the proposed solution is to utilize a commercially available switching-mode power supply (SMPS) with linear voltage regulator integrated circuits. A Mean Well RT-65c triple output SMPS is selected for its small size, cost, better efficiency and

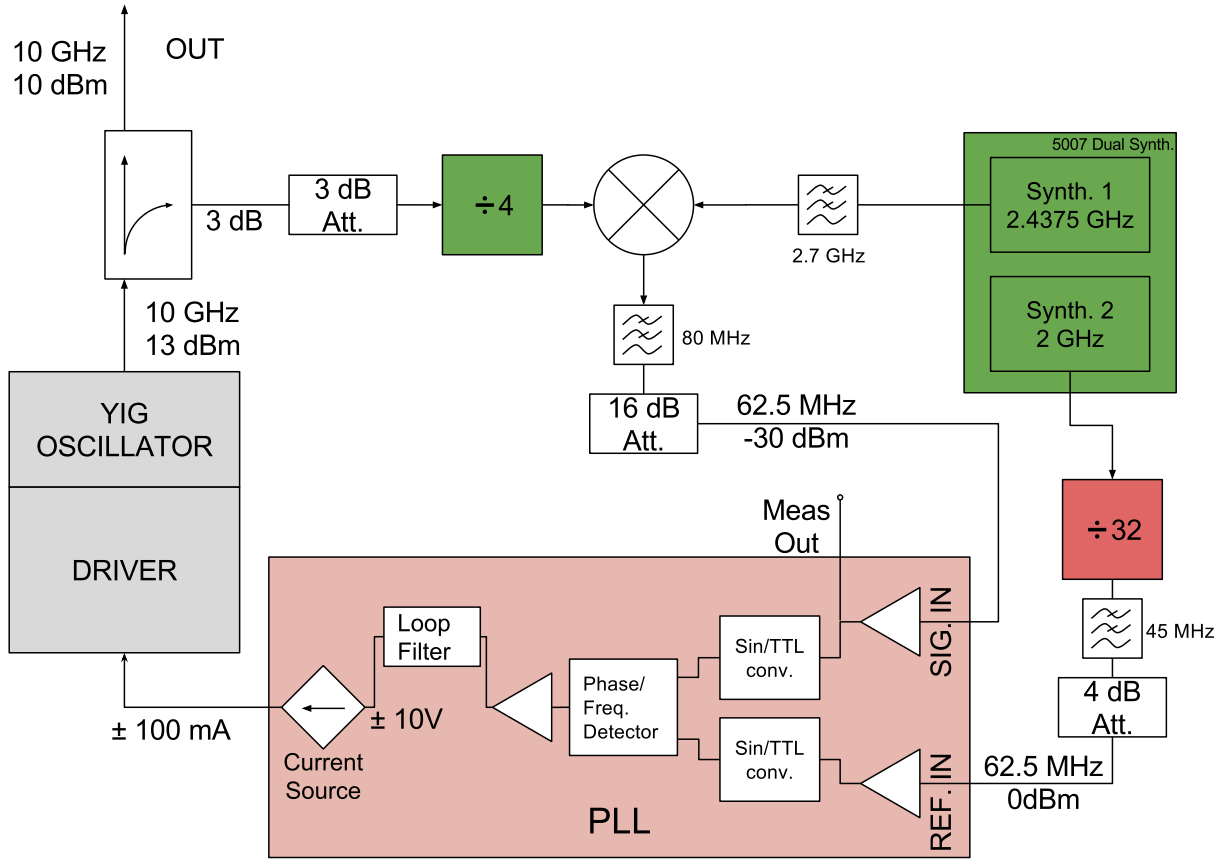


Figure 3.3: Simplified diagram of the YIG oscillator system.

Voltage [V]	Current [mA]	Power [W]	Devices powered
+5	800	4	Valon 5007, Valon 3008, HMC3625, PLL board
-5	300	1.5	PLL board
+12	260	3.12	YIG oscillator
-12	220	2.64	YIG oscillator
+15	200	3	PLL board (current driver)
-15	300	4.5	PLL board (current driver)
Total power		18.76 W	

Table 3.1: Power requirements for the YIG and control system.

availability. The main drawback of this power supply is the high-frequency noise it produces (around 100 KHz). It is transmitted through its output but also radiated. The most relevant characteristics of the SMPS are presented in Table 3.2.

To reduce the noise from the switching, linear voltage regulators and filters are used. As a first step in noise reduction, capacitors are placed in parallel to the outputs of the SMPS, working as low-pass filters. A second stage of noise reduction is implemented using linear voltage regulators from the L78xx and L79xx families of integrated circuits, as they have an important (>60 dB) ripple rejection. Unfortunately, it was not possible to implement the second stage to the ± 15 V lines because the linear regulators need to be supplied with a

	CH1	CH2	CH3
DC voltage	5 V	12 V	-12 V
Current range	0.5 ~ 8A	0.2 ~ 3 A	0~1A
Ripple & noise (20MHz bandwidth)	80 mVpp	120 mVpp	80 mVpp
Rated power	65.5W		
Efficiency (Typ.)	78 %		

Table 3.2: Most relevant electrical characteristics of the power supply.

voltage at least 2 V above its output (dropout voltage) and there was not an available SMPS that could supply this voltage.

The noise suppression is particularly relevant to the analog circuits and the YIG oscillator because noise in the supply lines is easily transferred to the signals. In particular, the YIG oscillator requires a noise below 10 mVpp from 2 kHz to 3 MHz. It is also important to note that the PLL board does not have a direct GND connection in its supply pins, it is grounded only through the SMA connectors.

3.1.2. Laser coupling into a single-mode fiber

The original fiber-coupler of the laser has a built-in isolator that prevents backreflections to the cavity, but for this case it also prevents the injection of an external signal. In order to remove the isolator that prevented the injection of a signal into the internal cavity of the slave laser, the original coupling system had to be removed. Therefore, a new optical system was implemented to couple the free-beam output of the laser into a mono-modal optical fiber. Observation of the output beam using viewer cards showed that the beam is astigmatic and that it doesn't change its profile considerably in the first 80 cm. Considering this, an optical system was designed. A Thorlabs F280APC-1550 fiber collimator is selected to couple the beam into the fiber and a pair of plano-convex cylindrical lenses correct the beam's astigmatism. The lenses have foci of 15 and 40 mm and are placed to enlarge the beam's profile in the direction perpendicular to the floor, as seen in Figure 3.4.

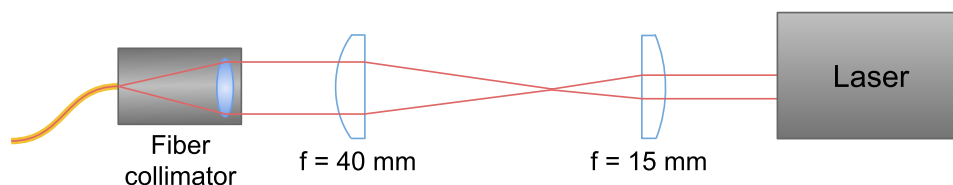


Figure 3.4: Optical diagram of the fiber coupling optics. Not to scale.

These optical components need a mechanical mounting system that allows precise tuning and good stability. Various schemes were tested. The first mounting system was implemented using separate pole mounts for each component over a self fabricated optical table, but the optical table was easily bent and each component had many degrees of freedom, which resulted in bad stability and very difficult alignment. As an alternative, a custom 3D printed

plastic block was design and tested but it was also discarded because the fabrication process was difficult and the tuning capabilities where insufficient.

Finally, an optomechanical 30 mm cage system was selected, with two cylindrical lens mounts and one kinematic mount for the collimator, all fabricated by Thorlabs. The cage system is mounted with two poles to a small optical table to which also the laser head is mounted. By changing the height of the poles and their position on the optical table, the cage system is aligned to the optica axis of the laser (Z axis). Then, the cylindrical lenses can be translated along the Z axis to adapt the beam shape. At the end, the tip-tilt adjustment of the collimator is realized with a kinetic mount. The system is shown in Figure 3.5.

The efficiency of the coupling was measured by dividing the coupled power in the fiber by the total power from the output beam, as seen in equation (3.6). This was measured with an optical power meter with a fiber and a free-beam sensor. The maximum measured coupled power was 3 mW, but the typical operation value was 2.6 mW.

$$\text{Typical coupling efficiency} = \frac{\text{Power in fiber}}{\text{Total output power}} = 65 \% \quad (3.6)$$

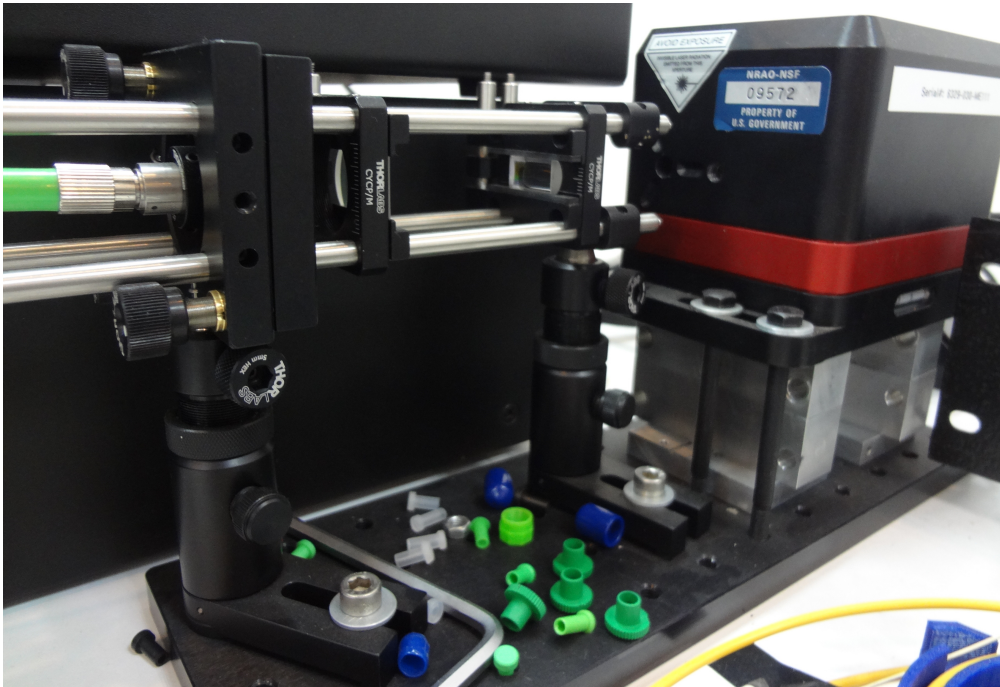


Figure 3.5: Fiber-coupling of the diode laser with the cage assembly.

3.1.3. Injection locking

The slave laser is constructed using a modified Littman-Metcalf cavity, with a diffraction grating working as a spectral bandpass filter with a couple of gigahertz bandwidth. The cavity can be coarse tuned using a DC motor and fine tuned with a piezo actuator. The

cavity is specially designed to tune the frequency of operation without mode hops. With a coarse tuning range of almost 200 THz and fine tuning range of 30GHz [31], the slave laser can be easily tuned inside the locking range.

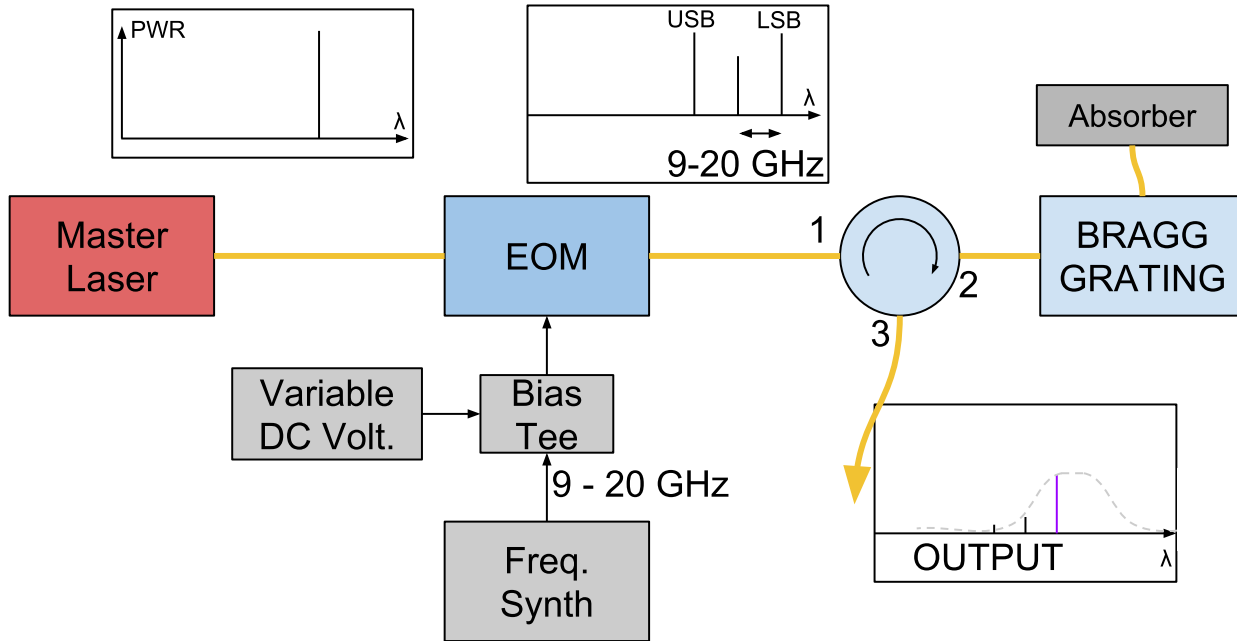


Figure 3.6: Diagram showing the process to generate the continuously tunable infrared signal for the photomixer. A laser is amplitude-modulated with a variable frequency from 10 to 20 GHz. The lower side band produced by the modulation is then extracted using the reflective properties of a fiber Bragg grating and an optical circulator.

3.2. Small range, continuously tunable signal

To generate an infrared signal with at least 10 GHz of tunability range a system based on an electro-optic modulator (EOM) is proposed. A diagram of the proposed system is depicted in Figure 3.6. The strategy is to modulate the amplitude of the master laser to generate sidebands spaced between 9 and 20 GHz from the carrier and then suppress one of the sidebands and the carrier signal. The system is integrated inside a 1U rack and an independent power supply is being designed for it.

3.2.1. Amplitude modulation

The amplitude modulation is achieved using a Lithium Niobate Electro-Optic Modulator. It uses an integrated Mach-Zehnder configuration to convert single polarization continuous-wave light from a semiconductor laser into a time-varying optical output signal [36]. The modulator uses an external RF source to change the relative phase between the signals of the arms of the interferometer. An optional DC bias voltage can be supplied to introduce an offset to the modulation.

3.2.2. Sideband and carrier suppression

Only one of the sidebands is desired and therefore the other must be suppressed as well as the carrier. For filtering, a fiber Bragg grating (FBG) is chosen. The lower sideband is placed on the reflective band of the FBG and the other signals are mostly transmitted. To retrieve the reflected signal an optical circulator is placed between the EOM and the FBG. This configuration was chosen (instead of selecting by transmitting only one sideband and reflecting the other modes) because the reflection curve is more stable in the desired band (see Figure 3.7).

To optimize the selectivity, the master laser is thermally tuned so that the LSB is located in the reflection band as close to the edge as possible (purple markers in Figure 3.7). This means that the laser should be set to radiate at 1555.8677 nm considering a fiber with refractive index of 1.45 (red marker). The expected values of attenuation are shown in Table 3.3.

	Attenuation
Carrier	18.2 dB
LSB	4.7 dB
USB	>30 dB

Table 3.3: Expected attenuation after retrieving the reflected signal from the FBG, considering attenuation produced by the optical circulator.

Besides the use of the FBG, it is important to adjust the bias voltage of the EOM to suppress the carrier and increase the magnitude of the modulation.

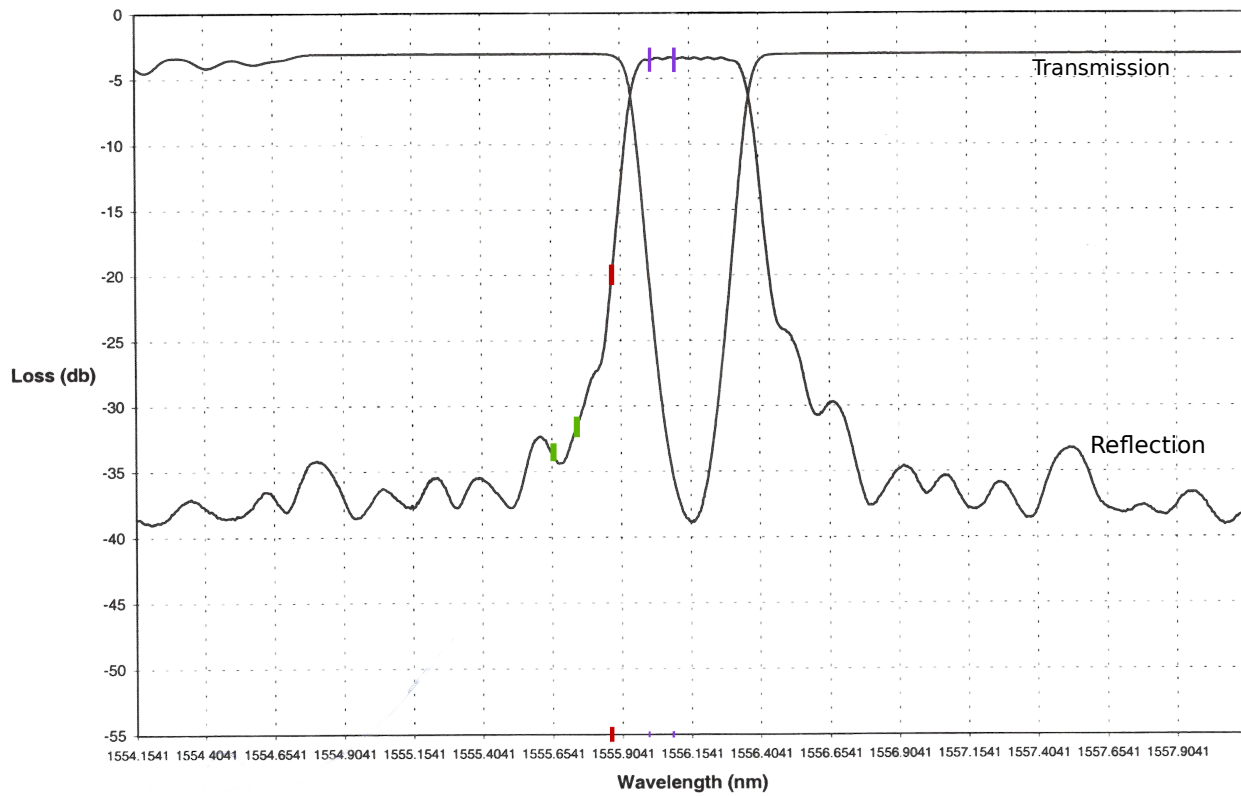


Figure 3.7: Transmission and reflection curves of the fiber Bragg grating (FBG) used. The desired operation point of the laser is marked with red. The USB and LSB ranges are denoted with the green and purple dots, respectively [32].

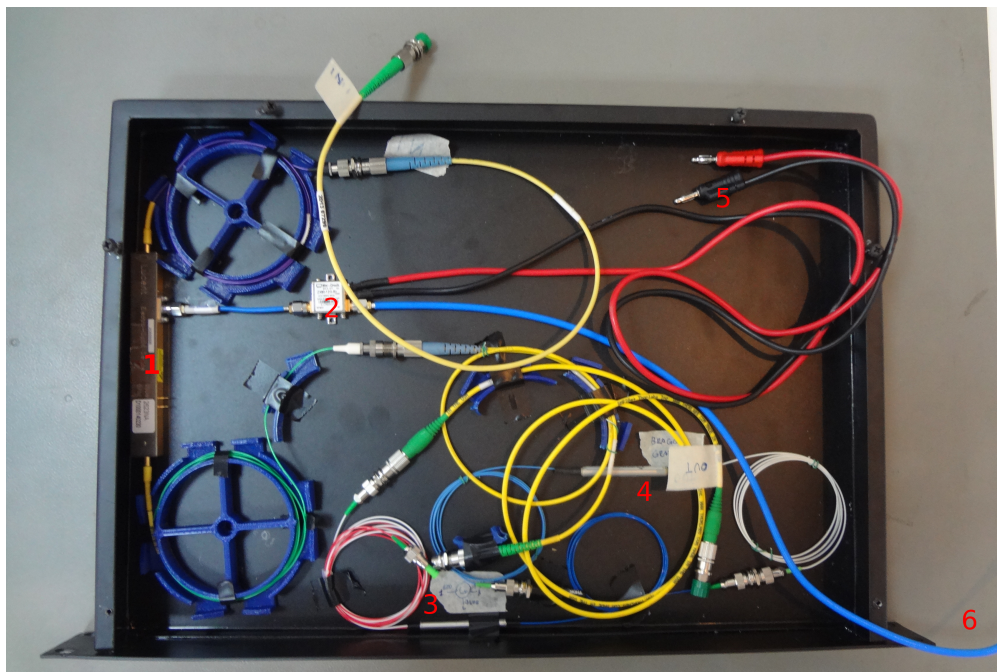


Figure 3.8: Continuously tunable signal synthesizer. 1: EOM, 2: Bias tee; 3: Optical circulator, 4: Fiber Bragg grating, 5: Bias DC input, 6: RF input.

Chapter 4

System Evaluation

4.1. Discrete tunable signal synthesis

4.1.1. YIG oscillator as a reference signal

To use the YIG oscillator as a reference, it is required that its signal is highly stable, have minimum spurious signals and low phase noise.

The YIG oscillator delivers a signal with phase noise below -60 dBc and harmonics below -12 dBc according to the measurements taken. The main problem with this oscillator is its frequency drift (Figure 4.1, blue line). According to the original calibration test from the manufacturer, the free-running frequency of the device is 10.003 GHz but the measurements made show that the output frequency varies with the temperature of the device and takes more than three hours to stabilize. This was observed by measuring the temperature at the case of the device and measuring the peak frequency observed with a spectrum analyzer.

The phase-lock loop control system implemented should be able to maintain the device oscillating at 10 GHz, countering the thermal drift and other faster perturbations. Nevertheless, initial measurements with the control system show that it adds noise to the oscillator and lowers its frequency by a constant value, as seen in Figure 4.2. As the oscillator's frequency is shifted only by a fixed value, thermal drift is not compensated (Figure 4.1). The control system is highly sensitive to noise and good grounding is vital.

As the control system was not performing as it should, it was studied to correct possible errors. The first step was to disassemble the system and study each one of the devices involved: dual synthesizer, mixer, frequency dividers (see Figure 3.3). The oscillator used in the mixing (Synth. 1 from Figure 3.3) was found to be configured at a wrong frequency so it was reprogrammed. Also, to reduce its harmonic noise a low pass filter was added at its output. Another filter was placed at the output of the divide-by-32 frequency divider. Attenuators were used to adjust the power level in order to match the design levels of the PLL board.

The system was reassembled and tested, but the same problems continued. It was then

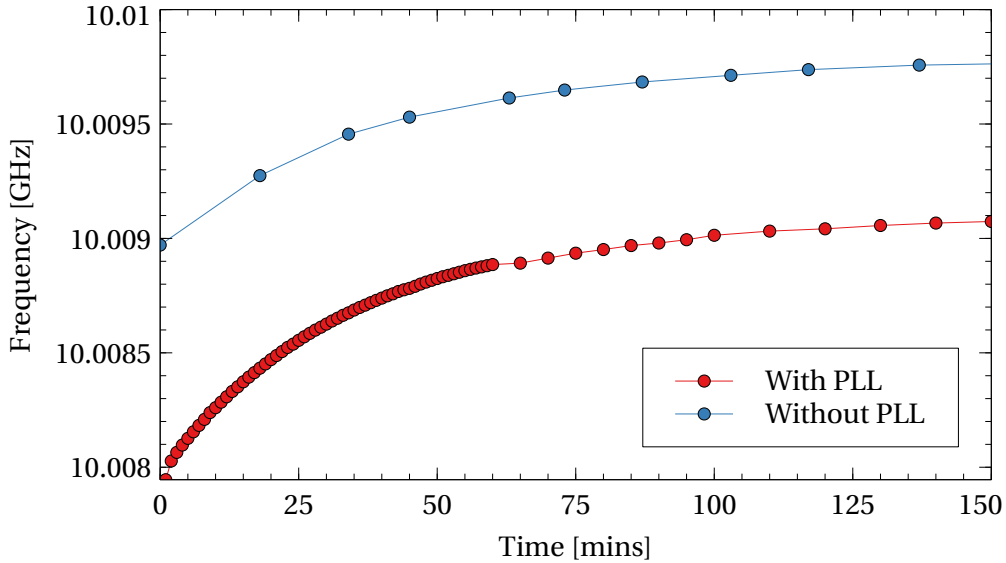


Figure 4.1: YIG oscillator frequency drift with and without the PLL control system.

presumed that the problem is in the PLL board as all the rest of the system worked. Every stage of the process that occurs in this board is tested. These stages are: pre-amplification of the input signals, sinusoidal-to-TTL logic conversion, comparison of the frequencies, amplification, filtering and finally the voltage signal is transformed into a current signal. A more detailed description can be found on [29].

To study the PLL board, both of its inputs were connected to a function generator. This helped to rule out possible errors carried in by other devices. With the first observations, it was evident that the electrical grounding of the board is critical. The pre-amplification stage worked correctly for both of the input channels, but it was observed that the reference signal's amplitude is modulated by a 350 Hz signal, independently of the source of the 62.5 MHz reference. After the amplification, both signals are transformed to almost-square signals (Figure 4.3). At this point, both signals have the same amplitude.

The output of the AD9901 discriminator changes with the frequency difference between the input signal and the reference accordingly to the documentation of this component. The differential amplifier that is placed after discriminator also performs as expected.

The loop filter should transform the output signal of the discriminator, a square signal, into a DC signal of which the voltage level is proportional to the frequency difference at the input of the discriminator. This signal should have a range between -10 and 10 V. However, the measurements show that the signal is a constant DC component and another smaller variable signal over it. This explains why the YIG is tuned always with a constant value when it is connected to the PLL board. Figure 4.4 shows the signal after the filter when the frequency difference is 10 MHz.

To study the capacity of the PLL board to drive the YIG oscillator, the input signal is set at different frequencies with the function generator. When the frequency is set to be the same as the reference signal (62.5 MHz), the YIG oscillator shouldn't be affected, but

when there is a mismatch between both frequencies, the control system should drive the YIG frequency proportionally. Figure 4.5 shows that the PLL board fails to drive the YIG frequency correctly, as the center frequency remains the same under all the conditions and the signal is only distorted.

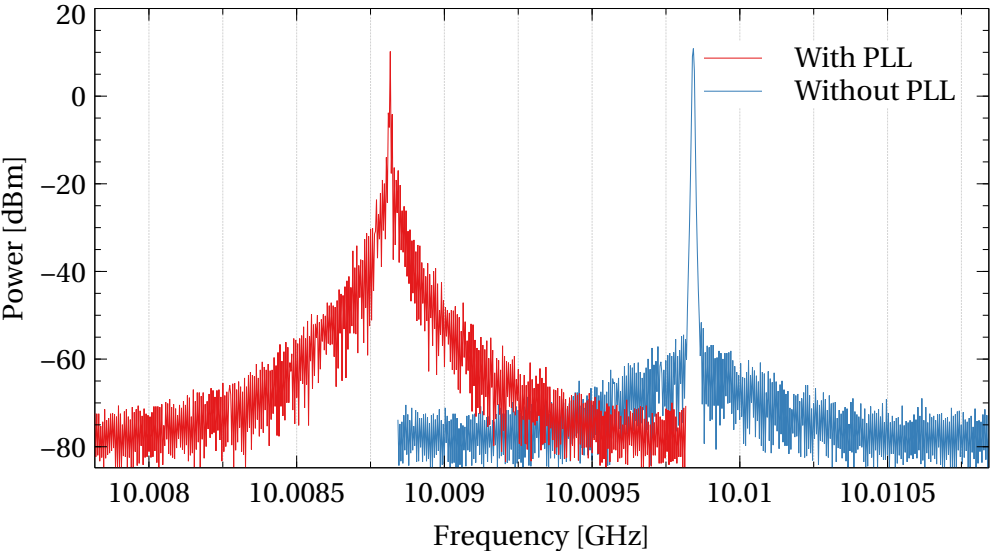


Figure 4.2: YIG oscillator's output spectrum with and without the PLL control system.

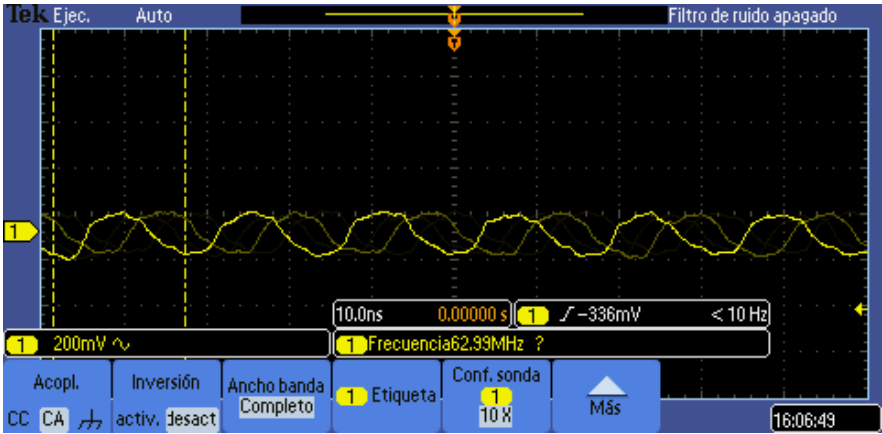


Figure 4.3: Signal after the sinusoidal-to-TTL conversion in the PLL board.

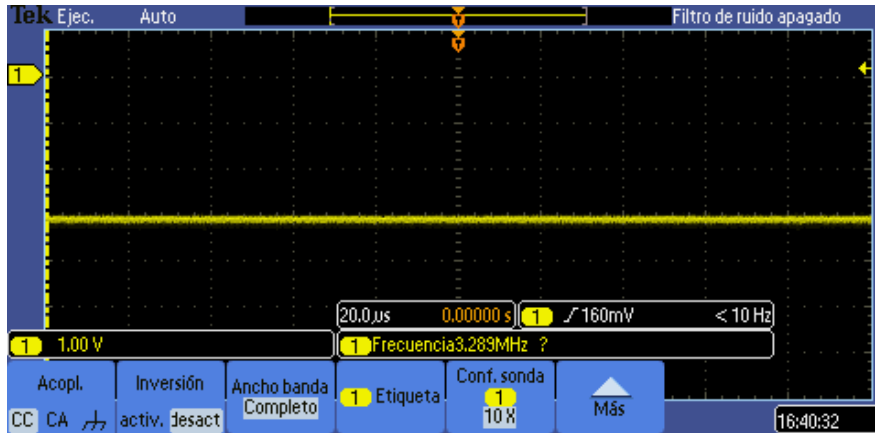


Figure 4.4: Signal measured after the loop filter in the PLL board. Difference of frequency between input and reference is 10 MHz.

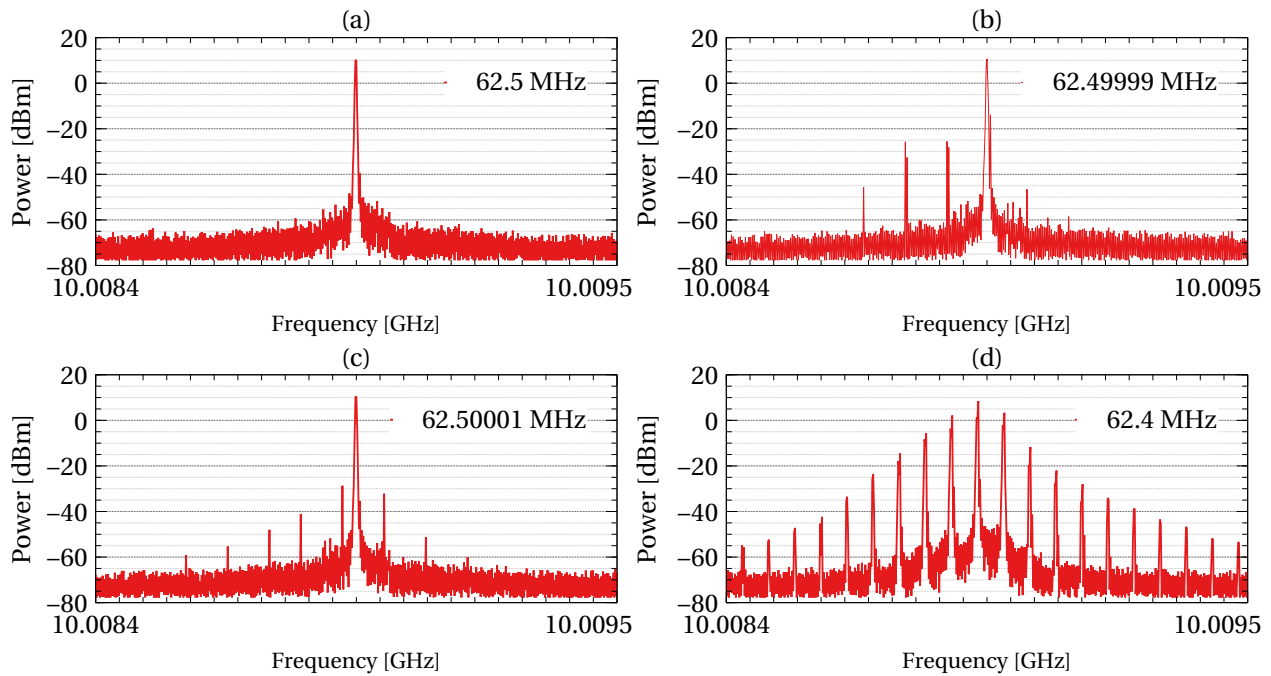


Figure 4.5: YIG driven by PLL with different input signal's frequency. The reference signal is 62.5 MHz.

4.1.2. Optical frequency comb generator

The purpose of the comb generator is to produce the signals that are injected to the slave laser. Because of this, the most relevant parameters to evaluate the performance of the comb generator are:

- Comb lines' span: number of comb lines available and their power distribution.
- Efficiency: output power of the comb with respect to its input optical power.
- Stability

To study the comb generator's behavior, its output is connected to an optical spectrum analyzer. As the YIG oscillator is not frequency-stable nor amplitude-configurable, a RF frequency synthesizer is used instead to drive the comb generator. The Koheras fiber laser is used as the optical input.

The comb generator's optical efficiency is highly dependent on the polarization of the optical input signal. By adjusting the manual polarization controller and with the RF signal off, the peak of the output was observed to vary between 7.5 nW and 216 nW for different polarizations when the input was 27.66 mW, as measured with an optical power meter. This accounts for a gain of -51 dB in the best case. Figure 4.6 shows the optical input and output relationship obtained with the best polarization, measured with an optical spectrum analyzer.

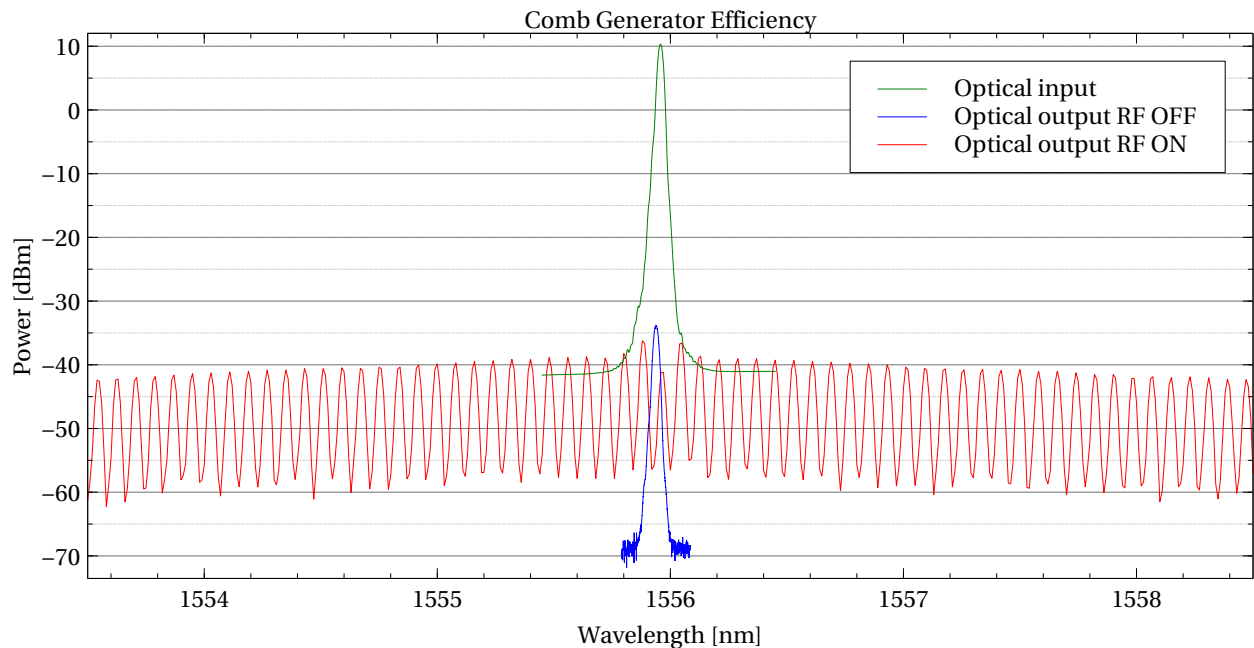


Figure 4.6: OFCG input and output power, with RF input signal on and off.

Besides input polarization, the main variables that affect the output of the comb generator are: optical input power, RF input power and bias voltage. Each of these variables affect the output of the device. Under normal operation, optical and RF power are set and then the voltage is adjusted to get the desired output.

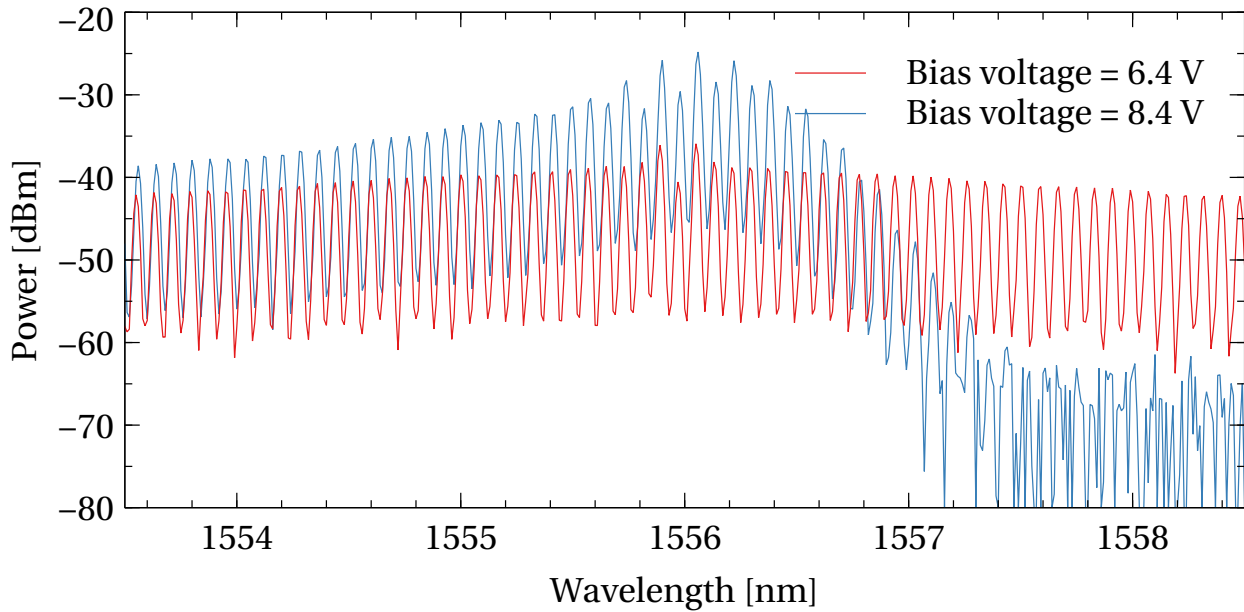


Figure 4.7: OFCG output with two different bias voltages.

Figure 4.7 shows the variation in the balance of the comb lines for two different bias voltages. The power of the comb lines is not always symmetric with respect to the center frequency and the comb flatness can be increased or decreased. The curves shown are not stable on time and to maintain them certain adjustments to the bias voltage have to be made. Figure 4.8 shows the variation in the output when the optical input power is changed. It is not possible to find a optimal point of operation (RF input power, optical input power, bias voltage) because the output is variable and the results are not reproducible. The suspected origin of this undesired behavior is thermal instability.

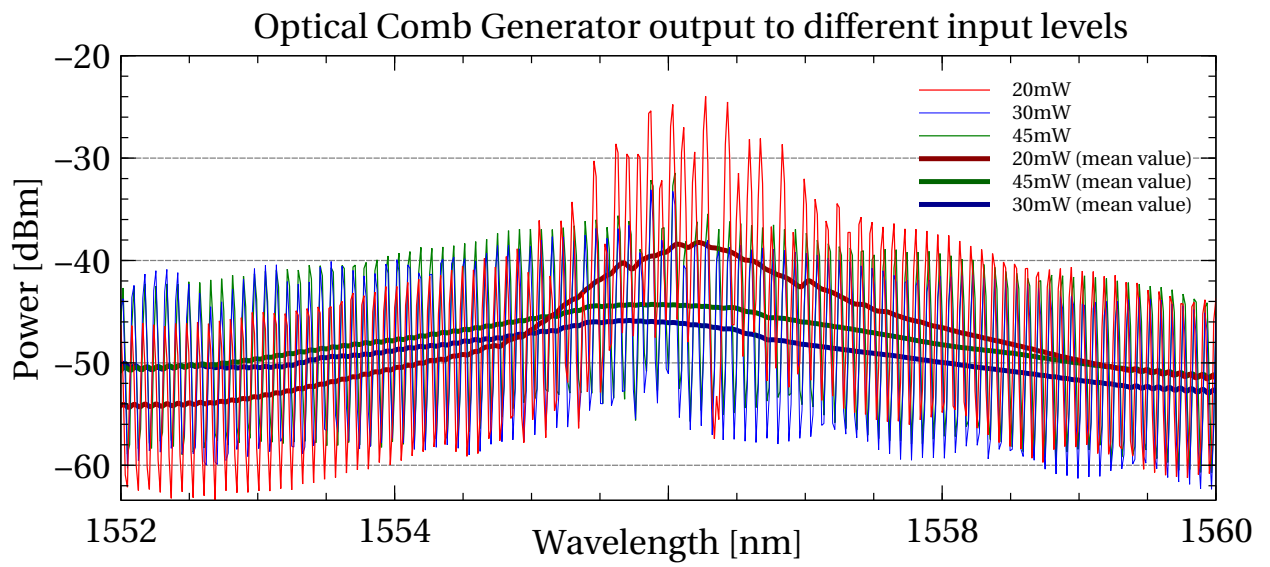


Figure 4.8: OFCG output to different input levels. The input levels correspond to the laser setpoint.

4.1.3. Injection locking

The injection locking measurements are taken by mixing the master laser and the slave laser in a fast photodiode. The electrical signal is amplified with a low noise amplifier (LNA) and then observed in an electrical spectrum analyzer (ESA) as shown in Figure 4.9. The amplifier has a frequency range of 1-12 GHz which limits the range of observation. The slave laser has been successfully locked to the first upper and lower sideband (± 10 GHz). Injection locking to higher comb lines has not been observed as the beat of the two lasers is outside the amplification range of the LNA.

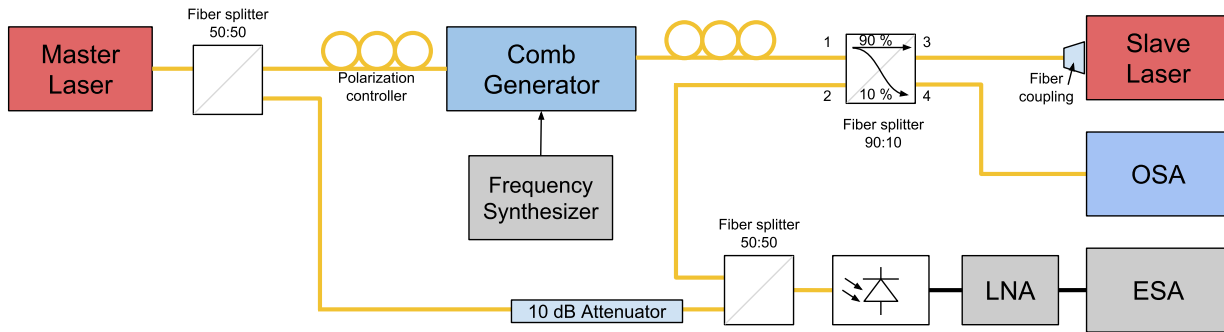


Figure 4.9: Setup for measuring the injection locking. The optical spectrum analyzer is used to monitor the comb lines while the electrical spectrum analyzer is used to observe the locking.

Figure 4.10 shows the beating of both lasers as the slave laser is brought closer to one of the comb lines. The highest peak is the beat between the two laser.

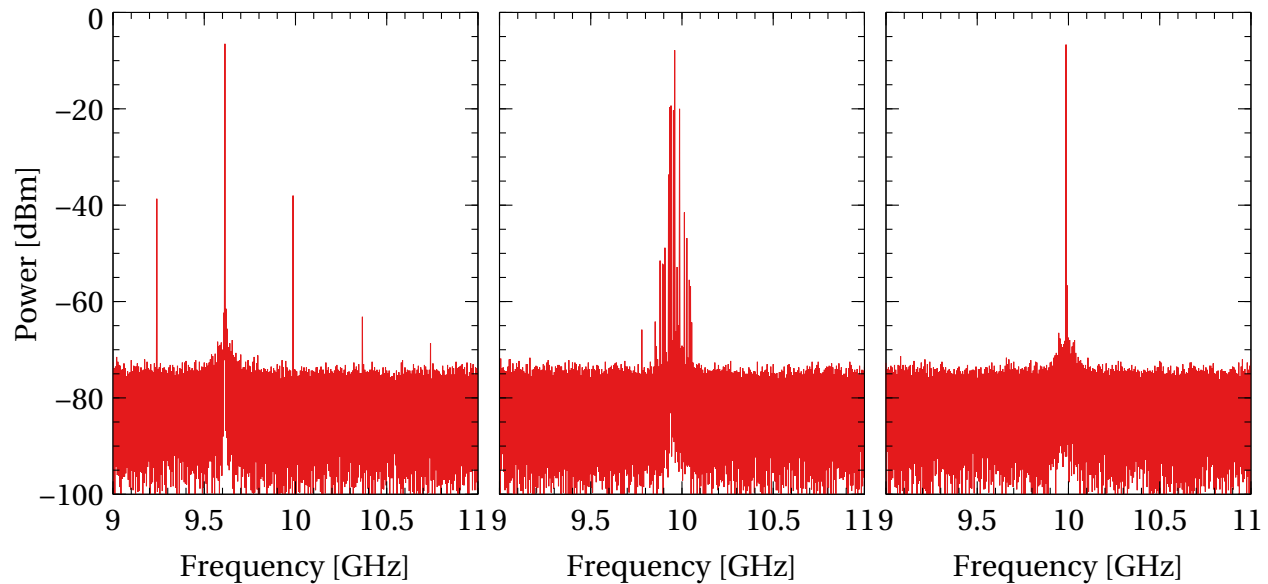


Figure 4.10: Three phases of the slave laser (SL) locking to the comb line. Left: SL far from the locking range. Middle: SL very close to the locking range. Right: SL injection-locked.

To study the long term stability of the locking, the beating was observed with the ESA

on ‘max hold’ function. Two cases are compared. In the first case, the slave laser is injection-locked just before the measurements take place. In the second, the optical input of the comb generator is unplugged and the slave laser is tuned to lase 10 GHz above the master laser and then left free-running. The OFCG is supplied with 38 mW of optical power. The RF power is set to -5dBm and the diode laser’s current is set to -55.4 mA. The comb line injected has an estimated power of -40 dBm ¹.

Figures 4.11 and 4.12 show the results for the first 75 minutes. It can be seen that within the first 5 minutes the slave laser remained locked, but in the next 5 minutes, one ‘hop’ or jump outside locking occurred, which considerably expanded the width of the line. One cause of this could be mechanical perturbations of the setup. During the next 20 minutes, up to the 30 minutes of the experiment, no further increase in the line is seen, so it can be inferred that no other hops occurred on this period, or they where smaller the first one. In the last minutes of the experiment the slave laser became unlocked. On the top graph of Figure 4.11, which corresponds to observed signals without ‘max hold’ function, the free-running case is seen at its final position (after 75 minutes).

¹It is not possible to measure it directly.

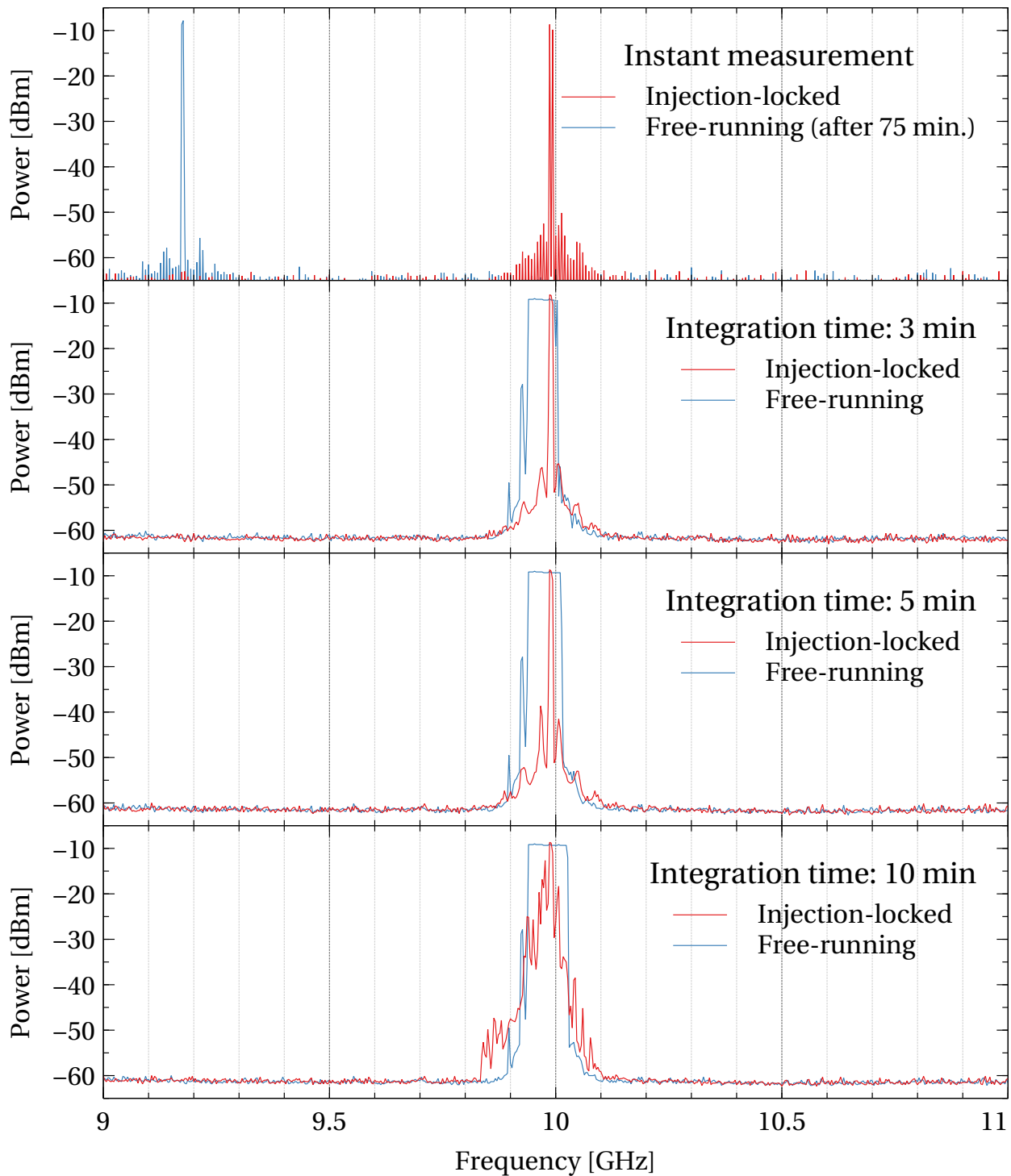


Figure 4.11: Comparison of the beating between both laser on a photodiode, with the slave laser locked at the first comb line (blue) and with the slave laser free-running at an initial distance of 10 GHz from the master laser (red). The spectrum analyzer was on 'max hold' function during 15 minutes.

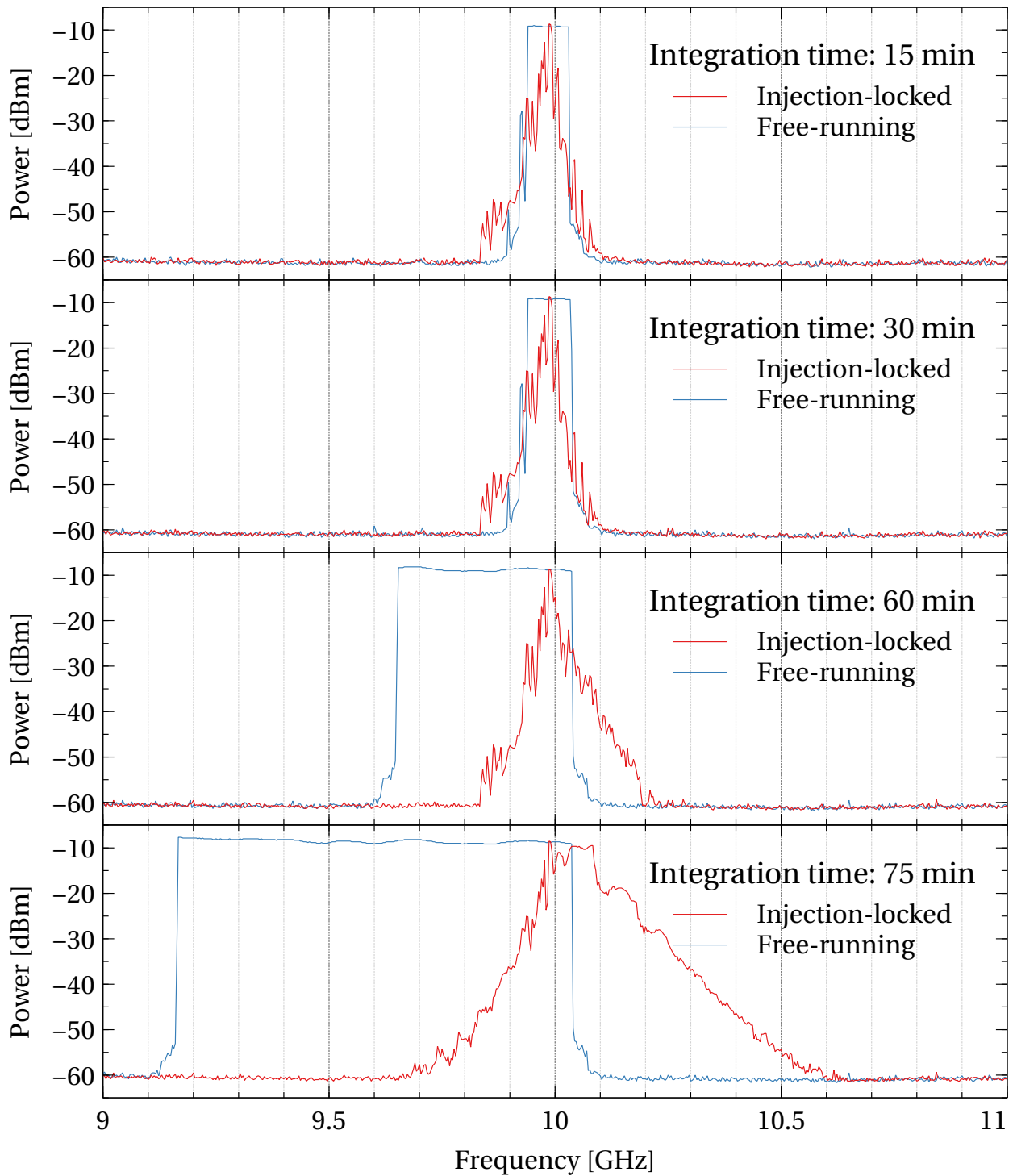


Figure 4.12: Comparison of the beating between both laser on a photodiode, with the slave laser locked at the first comb line (blue) and with the slave laser free-running at an initial distance of 10 GHz from the master laser (red). The spectrum analyzer was set to *max hold*.

4.2. Continuously tunable signal synthesis

To measure the capabilities of the proposed system to generate and isolate a continuously tunable signal, the EOM is fed with the Koheras laser (ML) and modulated using a frequency synthesizer and adjustable DC power supply connected to a bias tee. The output of the system is observed on an optical spectrum analyzer.

4.2.1. Amplitude modulation

The first measurements taken have the objective of studying the EOM. With this purpose the output of this device is connected directly to the ESA, bypassing the bragg grating. To find the best operational point, the effect of the bias voltage and the modulation RF power on the levels of the sidebands and the carrier are studied.

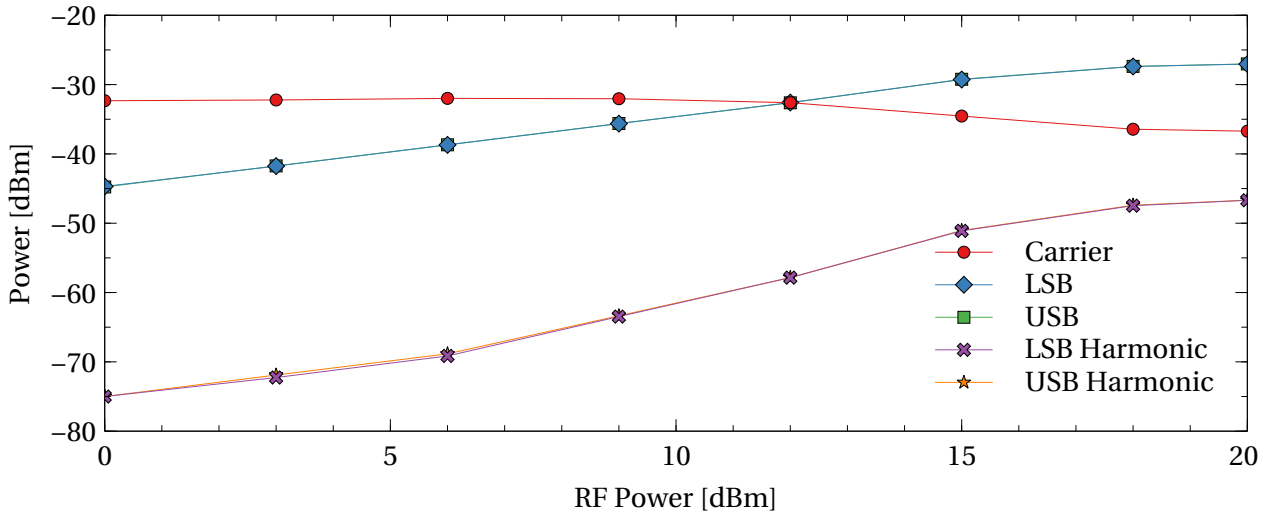


Figure 4.13: Output power of the carrier, sidebands and harmonics versus input RF power.

In Figure 4.13, the laser is set to a wavelength of 1555.93 nm and 10 mW output power. The bias voltage is set to 4.1 V as this was previously found to be the point at which the carrier was attenuated the most. It is observed that the sidebands are symmetric (hence they are superposed on the graph) and that with higher RF power, harmonics of the sidebands appear.

After the initial study of the effect of the bias voltage, the analog power supply was replaced with a more precise digital one. The voltage was scanned on the -15 to 15 V range with 0.5 V steps. Figure 4.14 shows the results for a 9 GHz modulation with 15 dBm. The experiment was repeated with 20 GHz and showing very similar results.

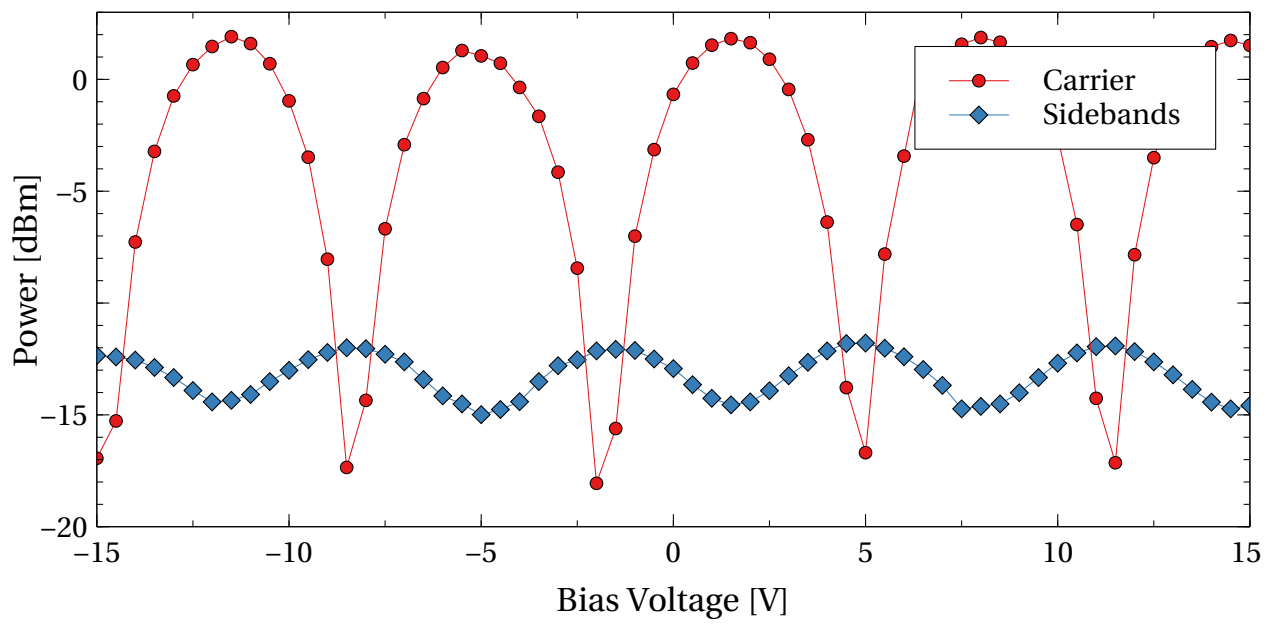


Figure 4.14: The effect of varying the DC bias voltage in the power level of the carrier and sidebands of the amplitude-modulated signal.

4.2.2. Sideband and carrier suppression

The Bragg grating is highly sensitive to the wavelength. This requires that the laser is tuned precisely thus the lower side band is placed in the reflected section while carrier and upper side band are mostly transmitted. The wavelength was calculated using the Bragg grating's datasheet, but when the laser was set to the calculated wavelength, the results were not the desired. Therefore, different wavelengths were tested to find the best operation point. Figure 4.15 shows the results of the sidebands and carrier levels of the modulated signal after being reflected on the Bragg grating. The laser is set to 10 mW, the bias voltage is 4.1V and the RF power is 17 dBm.

To measure the isolation of the LSB, the relative power of the LSB with respect to the next most powerful signal is calculated. The results are shown in Figure 4.16. The worst results are shown in the lower frequencies, 10 - 13 GHz, for all wavelengths, because of the high level of the second harmonic. After 14 GHz, the second harmonic starts to fade. Between 14 and 19 GHz the LSB is more stable and isolated.

While it is important to separate the desired signal (LSB) from the others, it is also important to maintain high and stable power. Table 4.1 shows the mean value and variance of the LSB for each laser setting. At wavelengths of 1555.93 nm and 1555.94 nm the LSB has its maximum mean value, and its minimum variance is at 1555.93 nm.

ML Wavelength [nm]	LSB Mean [dBm]	LSB Variance
1555.91	-39.97	7.658
1555.92	-38.87	8.985
1555.93	-37.47	6.712
1555.94	-37.30	7.027

Table 4.1: Mean value and variance of the LSB with the master laser set to different wavelengths.

From the studied wavelengths, 1555.93 nm shows the best overall results considering the mean value, power variation of the LSB for different modulation frequencies and rejection of spurious signals.

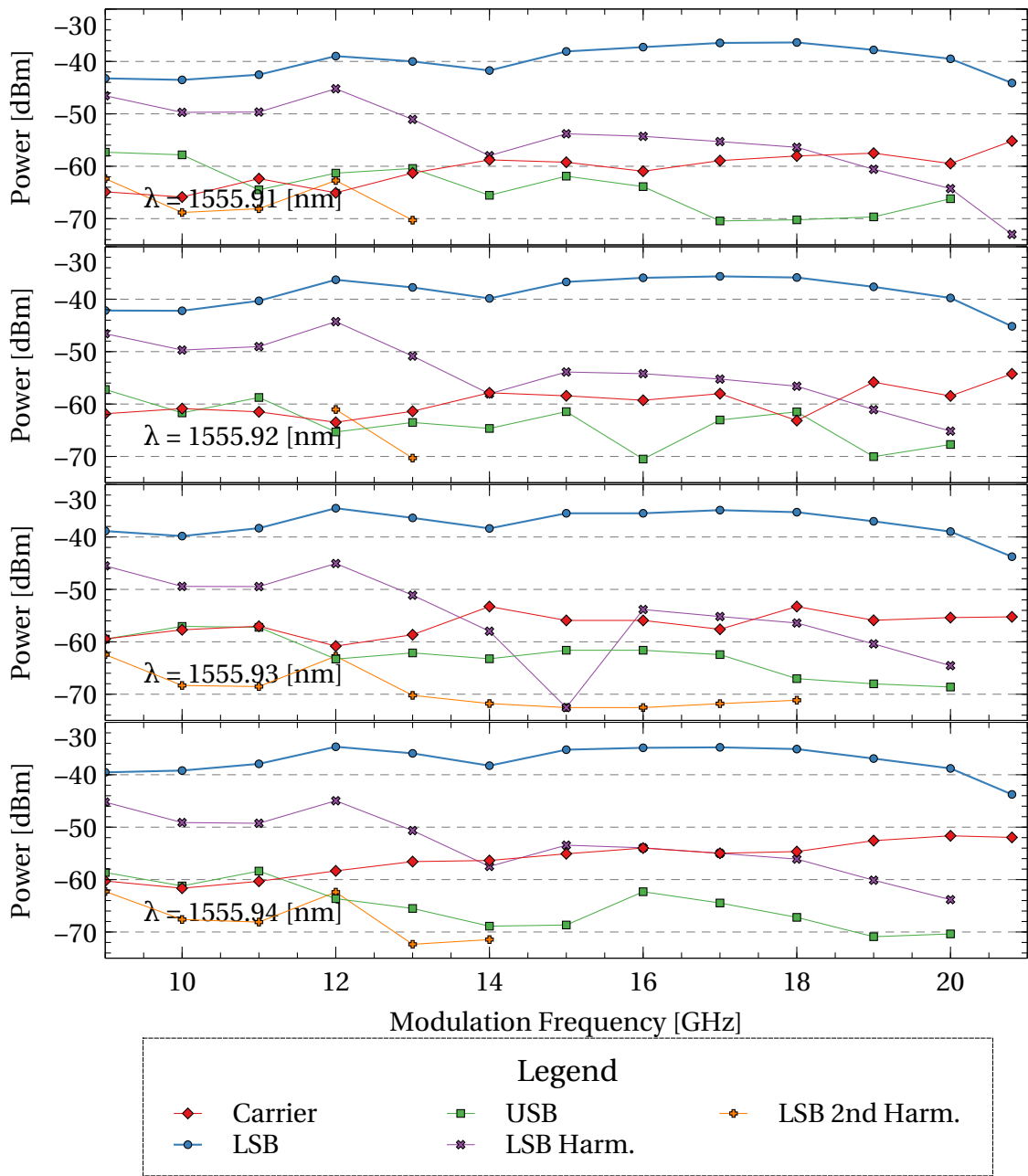


Figure 4.15: Sideband and carrier (laser) levels for different modulating frequencies and laser wavelengths. The sideband that is desired to extract (LSB) is in blue.

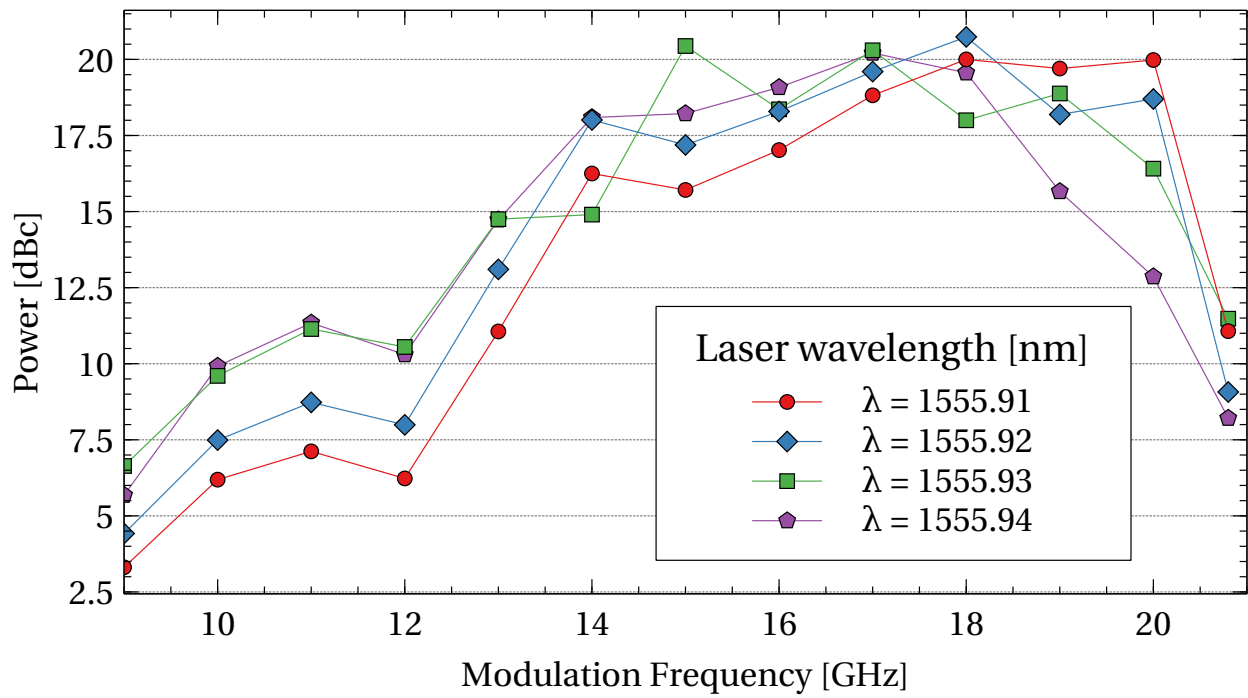


Figure 4.16: Relative power of the LSB with respect to the next most powerful signal at different modulation frequencies and laser wavelengths (λ).

Chapter 5

Conclusions and Future Work

5.1. Conclusions

With the conducted experiments, it is possible to conclude that both synthesis processes can be done with the conceived design. It was not possible to evaluate both subsystems in conjunction because of the lack of a proper RF reference for the frequency comb, due to the poor performance of the YIG oscillator that had to be replaced by the RF synthesizer.

The subsystem designed to generate the discrete tunable signal was only evaluated with the slave laser locked to the first upper and lower comb lines, because of the limitations on the measuring system. However, there is no reason to assume that the observed results are not reproducible for other comb lines. The main requirement for stable injection locking is the stability of the power of the comb lines.

The continuously tunable system has been proven to generate a signal with the proposed, design but shows very low optical-to-optical efficiency with deficient output power. At lower modulation frequencies, spurious signals can reach high levels and the desired signal's amplitude is variable in the studied range. Nevertheless, there is room for improvement of the system by better tuning of the many variables involved in the synthesis process and the addition of optical amplifiers. The characterization realized is adequate to give a general perspective of the behavior of the systems under different conditions that should be considered when setting the system for a precise point of operation.

5.2. Future Work

Many improvements to the system could (and should) be implemented. At first, a suitable reference source for the comb generator could be implemented if the PLL of the YIG oscillator is correctly repaired. It is also possible to use another control paradigm since the main problem is the slow thermal drift. Also, the comb generator stability could be improved by achieving better thermal stability. This will lead to longer injection locking times.

An optical circulator is an alternative to the 90:10 fiber splitter used to connect the optical comb with the slave laser. This would increase the output power at the expense of not being able to monitor the comb lines directly.

The continuously tunable signal needs an amplification stage to reach the output of the step-tunable laser, in the mw. Also, rejection of the other signals can be improved with proper tuning. For example, if the system is going to be operated modulating in a small frequency span, the RF power and even the master laser's wavelength can be changed to improve the purity of the signal.

Also, active suppression of the upper sideband could be conceived, taking into consideration a following second modulator which is fed by a properly amplified signal detected after the Bragg grating (replacing the absorber in Figure 3.6). Such a destructive interference scheme was demonstrated previously in this lab for laser noise-cancellation [33].

In addition, a dedicated high precision tunable voltage supply is being designed to be used for the bias voltage. Implemented, it will ease the operation of the subsystem. Once this task is completed, the subsystem can be finally integrated within a rack case for standalone operation.

Acronyms

AM Amplitude Modulation

BWO Backward-Wave Oscillators

DC Direct Current

EOM Electro-Optical Modulator

ESA Electrical Spectrum Analyzer

FBG Fiber Bragg Grating

FM Frequency Modulation

GND Ground

HEDY Huge Enourmous Distarter Yo'

LASER Light Amplification by Stimulated Emission of Radiation

LD Laser Diode

LNA Low-noise Amplifier

LSB Lower Side Band

ML Master Laser

OFCG Optical Frequency Comb Generator

OSA Optical Spectrum Analyzer

PLL Phase-Locked Loop

QCL Quantum Cascade Lasers

RF Radio-Frequency

SL Slave Laser

SMA SubMiniature version A – Connectors

SMPS Switching-Mode Power Supply

THF Tremendously High Frequency

TTL Transistor-Transistor Logic

TWT Traveling-Waves Tube

USB Upper Side Band

UTC Uni-Traveling-Carrier

YIG Yttrium Iron and Garnet

Bibliography

- [1] R. A. Lewis, “A review of terahertz sources,” vol. 47, no. 37, p. 374001. [Online]. Available: <http://stacks.iop.org/0022-3727/47/i=37/a=374001?key=crossref.1e26aa2d9d47555077630d2f1255f62e>
- [2] M. Fitch and R. Osiander, *Terahertz waves for communications and sensing*, vol. 25.
- [3] A. Y. Pawar, D. D. Sonawane, K. B. Erande, and D. V. Derle, “Terahertz technology and its applications,” vol. 5, no. 2, pp. 157–163. [Online]. Available: <http://linkinghub.elsevier.com/retrieve/pii/S0975761913000264>
- [4] W. S. Struve, *Fundamentals of molecular spectroscopy*. Wiley.
- [5] Y.-S. Lee, *Principles of terahertz science and technology*. Springer, OCLC: 254636760.
- [6] S. Preu, G. H. Döhler, S. Malzer, L. J. Wang, and A. C. Gossard, “Tunable, continuous-wave terahertz photomixer sources and applications,” vol. 109, no. 6, p. 061301. [Online]. Available: <http://aip.scitation.org/doi/10.1063/1.3552291>
- [7] M. Khabiri, “Characterization and analysis of continuous wave terahertz photomixers.” [Online]. Available: <http://hdl.handle.net/10012/6647>
- [8] NASA - peter siegel: Studying the energy of the universe. [Online]. Available: https://www.nasa.gov/audience/foreducators/k-4/features/Peter_Siegel.html
- [9] C. M. Armstrong. The truth about terahertz. [Online]. Available: <https://spectrum.ieee.org/aerospace/military/the-truth-about-terahertz>
- [10] What is a gyrotron? – bridge12. [Online]. Available: <http://www.bridge12.com/what-is-a-gyrotron/>
- [11] Radar basics - extended interaction klystron. [Online]. Available: <http://www.radartutorial.eu/08.transmitters/Extended%20Interaction%20Klystron.en.html>
- [12] B. E. A. Saleh and M. C. Teich, *Fundamentals of photonics*, 2nd ed., ser. Wiley series in pure and applied optics. Wiley Interscience.
- [13] X.-C. Zhang and J. Xu, *Introduction to THz wave photonics*. Springer, OCLC: ocn428029012.

- [14] A. R. Lavado, "Covering thz gap using photomixers technologies: Arrays and new antenna topologies."
- [15] E. Pliński, "Terahertz photomixer," vol. 58, no. 4. [Online]. Available: <http://www.degruyter.com/view/j/bpasts.2010.58.issue-4/v10175-010-0044-0/v10175-010-0044-0.xml>
- [16] V. H. C. Gil, "Electromagnetic and device simulations for improvements on vertically illuminated travelling- wave uni-travelling-carrier photodiodes."
- [17] T. Engel and P. Reid, *Quantum chemistry and spectroscopy*, 3rd ed. Pearson.
- [18] C. Melles Griot, *CVI Melles Griot : Introduction to Laser Technology*.
- [19] Encyclopedia of laser physics and technology - laser diodes. [Online]. Available: https://www.rp-photonics.com/laser_diodes.html
- [20] Encyclopedia of laser physics and technology - semiconductor lasers. [Online]. Available: https://www.rp-photonics.com/semiconductor_lasers.html
- [21] *A practical guide to handling laser diode beams*. Springer Berlin Heidelberg.
- [22] J. Mur, "Fiber lasers."
- [23] M. Wahlsten, "Phase-locking performance of optical injection-locking evaluated by coherent detection."
- [24] A. E. Siegman, *Lasers*. University Science Books, OCLC: 14525287.
- [25] N. Hoghooghi, "Injection-locked semiconductor lasers for realization of novel rf photonics components."
- [26] A. K. Pradhan and S. N. Nahar, *Atomic astrophysics and spectroscopy*. Cambridge University Press, OCLC: ocn664450708.
- [27] J. Tennyson, *Astronomical spectroscopy: an introduction to the atomic and molecular physics of astronomical spectra*, ser. Imperial College Press advanced physics texts. Imperial College Press ; Distributed by World Scientific Pub, no. v. 2, OCLC: ocn62024010.
- [28] *Fixed Frequency - Permanent Magnet Oscillator with FM Driver*.
- [29] *Diseño de la placa de oscilador local para el nuevo receptor del radiotelescopio Mini*.
- [30] *AD9901 Datasheet*.
- [31] *Model 6300-LN User's Guide*.
- [32] *Fiber Bragg Grating Inspection Report*.
- [33] E. A. Michael and L. Pallanca, "Broadband near-to-shot-noise suppression of arbitrary

cw-laser excess intensity noise in the gigahertz range,” *Opt. Lett.*, vol. 40, no. 7, pp. 1334–1337, Apr 2015. [Online]. Available: <http://ol.osa.org/abstract.cfm?URI=ol-40-7-1334>

[34] Manual fiber polarization controllers. [Online]. Available: https://www.thorlabs.com/newgrouppage9.cfm?objectgroup_id=343&pn=FPC030

[35] *KOHERAS ADJUSTIK Product Information Sheet.*

[36] *10 Gbits/s Lithium Niobate Electro-Optic Modulator.*

[37] *CTRC-15-3-FCA Optical Circulator Data Sheet.*

[38] *High Optical Power Handling Photodiodes to 50 GHz.*

Appendix A

Equipment

A.1. Lasers

A.1.1. Master laser

The Koheras AdjustiK E15 is a ultra low noise, single frequency and single polarization DFB fiber laser with active wavelength control and wide-range thermal wavelength tuning [35]. The most relevant specification can be seen in Table A.1 and Figure A.1 shows its appearance.



Figure A.1: Koheras AdjustiK E15 laser system [35].

Parameter	Specification
Center wavelength [nm]	1550
Line wigth [kHz]	<1
Output power [mW]	>100
Optical S/N [dB] (50 pm res.)	>50
RIN peak [kHz] @ 100 mW	>250
RIN level [dBm/Hz]	<-115 @ 1MHz/<-140 @ 10MHz
Thermal tuning range [pm]	>500
PM output	key aligned to slow fiber axis

Table A.1: Koheras AdjustiK E15 optical specifications [35].

A.1.2. Slave laser

The New Focus 6329 series External Cavity Tunable Diode Laser is a stable, narrow-linewidth source of tunable light. Its unique cavity design, based on the Littman-Metcalf cavity, assures continuous mode hop-free tuning. It can be tuned adjusting the angle of the tuning mirror, shown in Figure A.3. For the coarse tuning, the mirror is rotated with the DC motor. For the fine tuning, that movement is made with a piezoelectric transducer (PZT). The output power can be set by changing the diode current [31]. The laser systems consists in a laser head (seen in Figure 3.5) and a controller (Figure A.2). The main optical specifications can be found on Table A.2.



Figure A.2: Velocity 6300 control panel.

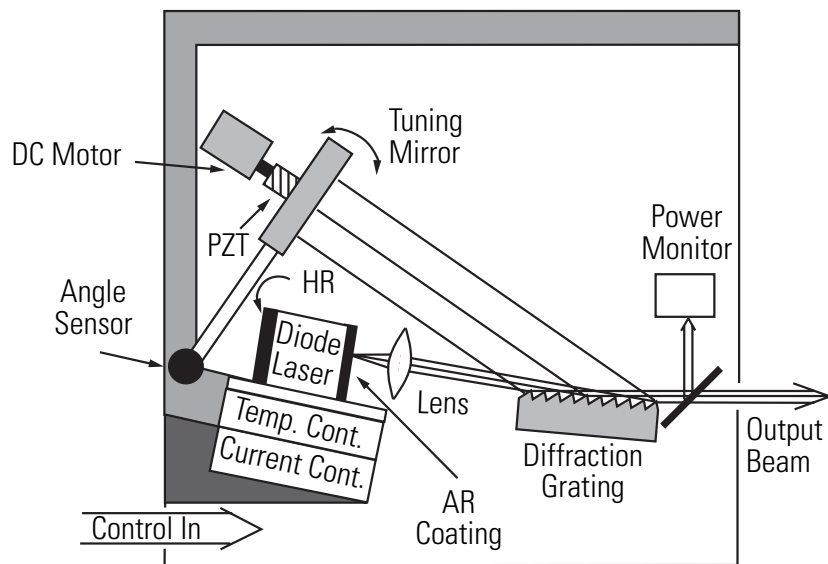


Figure A.3: Velocity 6300 laser head diagram [31].

Parameter	Specification
Center wavelength [nm]	1539
Linewidth [kHz]	<300
Output power [mW]	<25
Wavelength range [nm]	1496 - 1583
Fine frequency tuning range [GHz]	30
Coarse Tuning Resolution [nm]	0.02
Typical Wavelength Repeatability	>500
Fine-Frequency Modulation BW [KHz]	2
Current Modulation Bandwidth [MHz]	100

Table A.2: New Focus 63289 Velocity tunable diode laser optical specifications.

A.2. Optical equipment

A.2.1. Optical frequency comb generator

An optical frequency comb is a equally spaced series of lines in the frequency spectrum, hence the name. In the time domain, this is the equivalent of a regular train of very short pulses. The comb lines have the same amplitude and the spacing is usually in the range of 1 to 10 GHz. The frequency difference between the comb lines is equal to the inverse of the repetition time between the pulses.

There are different ways of producing an optical frequency comb. Optical frequency comb generators are electro-optical modulators that use a crystals to generate pulses from a coherent CW laser. The crystal is placed inside a resonant microwave waveguide, and the entire system is installed in a Fabry-Perot optical cavity. As the RF signal introduced to the waveguide modulates the refractive index of the crystal, the effective length of the optical cavity changes, hence the input laser radiation is periodically matched and miss-matched to the modes of the resonator, producing the pulsed radiation. A constant dc bias voltage can be applied to tune the crystal to a desired base state. The voltage required to induce a phase change of π is called the *half-wave voltage* (V_π).

The optical comb generator used, shown in Figure A.4, was constructed in the Terahertz and Astrophotonics Lab, using the OptoComb WR-100-03 modulator. The device includes a RF power amplifier, a tunable DC voltage supply and a temperature controller. It is designed to work with a CW coherent laser at 1556 nm and the optimal efficiency is achieved for 10 GHz modulation. The potentiometer on the front panel can be used to adjust the bias voltage.

A.2.2. Electro-optical modulator

The 2623NA 10 Gbits/s Electro-Optic Modulator is designed for long-wavelength, single-mode external amplitude modulation applications. It uses an integrated Mach-Zehnder con-



Figure A.4: Optical frequency comb generator

figuration to convert single polarization CW light from a semiconductor (DFB) laser into a time-varying optical output signal [36]. The device is seen in Figure 3.8. The main electrical and optical specifications are displayed in Table A.3.

Parameter	Specification
Operating wavelength [nm]	1525 - 1565
Insertion loss (typ) [dB]	3.7
Extinction ratio @ DC [dB]	27
Extinction ratio @ RF [dB]	13
Optical return loss [dB]	-35
Bandwidth [GHz]	10
Drive voltage (V_π) @ DC [V] (typ)	3.1
Drive voltage (V_π) @ 1 GHz [V] (typ)	4.1
Electrical return loss (10 GHz—18 GHz) [dB]	-8
Electrode impedance [Ω]	43
Max optimal input power [mW]	30
Max RF voltage (peak to peak) [V]	10
Max DC voltage range (RF input) [V]	-20 to 20

Table A.3: EOM electrical and optical parameters [36].

A.2.3. Fiber Bragg Grating

The implemented FBG is the FBG15-265-CV1B from JDS Uniphase. The reflection and transmission spectrum can be seen in Figure 3.7. A picture of this is in Figure 3.8.



Figure A.5: Manual fiber polarization controller. [34]

A.2.4. Optical circulator

The used optical circulator is the CTRC-15-3-FCA fiber three ports circulator. The circulator uses FC/APC connectors and the ports are identified with the fiber color: red = port 1, blue = port 2, white = port 3 [37]. The most relevant parameters can be found on Table A.4 and the device can be seen in Figure 3.8.

Parameter	Specification	Test Data
Operating wavelength range [nm]	1550 ± 20	1550 ± 20
Insertion loss (Port1 to Port2) [dB]	< 1.0	0.61
Insertion loss (Port2 to Port3) [dB]	< 1.0	0.67
Isolation (Port2 to Port1) [dB]	≥ 40	46
Isolation (Port3 to Port2) [dB]	≥ 40	44
Return loss (Port1) [dB]	≥ 55	59
Return loss (Port2) [dB]	≥ 55	56
Return loss (Port3) [dB]	≥ 55	59
Channel cross talk (Port1 to Port3) [dB]	≥ 50	55
Maximum Power Handling [mW]		500

Table A.4: Optical circulator specification and test data [37].

A.2.5. Manual polarization controller

The three-paddle fiber polarization controllers use stress-induced birefringence produced by wrapping the fiber spools to create independent wave plates that will alter the polarization of the transmitted light in a single mode fiber [34].

A.2.6. Photodiode

The Discovery Semiconductors DSC 20H is a high reliability, low harmonic distortion photodiode module designed for high optical power applications [38]. It is encased in a metal box as seen in Figure A.6. The main optical/electrical specifications can be found on Table A.5.



Figure A.6: Photodiode and low-noise amplifier (LNA) [38].

Parameter	Specification (Typ)
Usable spectral wavelength range [nm]	1064 - 1650
Responsivity @ 1550 nm [A/W]	0.70
NEP @ 300 K [pA/√HZ]	18
Ripple [dB]	± 1
3 dB Bandwidth [GHz]	35
Optical return loss [dB]	25
Bias voltage [V]	+5
1 dB Small signal compression @ 5V [mA]	13
Dark current @ 25 C, 5V [nA]	25
Input power damage threshold (peak) [dBm]	16

Table A.5: DSC 20H photodiode optical and electrical specifications [38].

A.3. Electrical equipment

A.3.1. YIG Oscillator

YIG oscillators are oscillators with very high Q characteristics and, in some cases, achieve a great tuning range. They are made of a Yttrium iron garnet sphere that resonates at RF frequencies when immersed in a magnetic field. The resonant frequency is proportional to the magnitude of the magnetic field.

The MLPF-1500FM is a YIG oscillator that includes a FM coil driver from Micro Lambda Wireless, Inc. The main electrical specifications are shown in Table A.6.

Parameter	Specification
Frequency range [GHz]	10.0
Power output [dBm]	13 Min
Free run accuracy [MHz]	± 20
Harmonics [dBc]	-12
Spurious [dBc]	-70
Phase noise @ 100 KHz [dBc]	<-120
FM sensitivity [MHz/V]	5.6
FM deviation [MHz]	± 56
Supply voltage [V]	± 12 to ± 15
FM tuning voltage [V]	± 10

Table A.6: YIG oscillator specifications.

A.3.2. Frequency synthesizer

The QuickSyn FSW-0020 microwave frequency synthesizer from Phase Matrix is a programmable oscillator with wide frequency coverage from 0.2 GHz to 20 GHz, sub-Hz resolution, instrument-grade spectral purity and compact size. The device provides AM, FM and phase modulation, as well as power leveling and control. The main parameters, according to the available datasheet are listed in Table A.7. It is important to note that the device operates outside those parameters, reaching frequencies up to 20.8 GHz and power up to 20 dBm. Also, the synthesizer can reach high temperatures if there is insufficient thermal dissipation.

Parameter	Specification
Frequency range [GHz]	0.2 - 20
Frequency resolution [Hz]	0.001
Power [dBm]	13
Power accuracy [dB]	± 2.0 typ.
Harmonics [dBc]	-35 typ.
Supply voltage [V]	+12 - +12.6

Table A.7: Frequency synthesizer main specifications.

A.3.3. Low noise amplifier

To amplify the signal from the photodiode, a ABL1200-08-3220 broadband low noise amplifier from Wenteq Microwave Corp is used. It features 1.0 to 12.0 GHz operation band and low VSWR. A picture of the the device can be seen in A.6 and a the main electrical specifications are displayed in Table A.8



Figure A.7: Microwave frequency synthesizer.

Parameter	Specification
Frequency range [GHz]	1.0 - 12.0
Small signal gain[dB]	32 (typ.)
Noise figure @ 25 C [dB]	2.0
Non-harmonic spurious [dBc]	-60 (max.)
Gain flatness [dB]	± 2.5 typ.
Supply voltage [V]	+8.0 - +12.0

Table A.8: LNA main specifications.

Appendix B

Operating Instructions

B.1. Discrete tunable signal synthesizer

You must be informed of the maximum ratings and operating instruction of all and each of the equipment used in the setup before using them. It is important to note that many of the devices implemented can be easily damaged by electrostatic discharges (ESD), exceeding maximum ratings or bad handling. Each of this devices has a proper instruction's manual or datasheet that has to be consulted.

To operate this subsystem, follow these instructions:

1. Connect the devices following diagram from Figure 4.9.
2. Disconnect the master laser from the system and turn it on.
3. Turn on the comb generator. Leave RF amplifier off.
4. Set the master laser power, make sure that less than 45 mW are injected to the comb generator.
5. Wait for laser and comb generator to thermally stabilize (3 hrs at least).
6. Set the frequency synthesizer to 10 GHz with less than 5 dBm of power. Leave output power off.
7. Turn on the RF amplifier from the comb generator.
8. Turn on the frequency synthesizer.
9. Connect the master laser.
10. Now, the comb lines should be visible in the OSA and the beating between the two laser should be visible in the ESA.
11. Adjust bias voltage and the polarization controller that is connected to the input of the comb generator to increase the power of the comb lines. To have a stable locking, it is recommended that the selected comb line's peak is seen in the OSA above -40 dBm, considering that the setup is the one depicted in Figure 4.9.
12. Place the slave laser over the desired comb line using the 'Wavelength Adjust' knob. To do so, you can use the OSA switching the observed signal, from the comb lines to

the slave laser.

13. Use the 'Piezo Voltage' knob to fine tune the slave laser into the locking range. Use Figure 4.10 as reference.

B.2. Continuously tunable signal synthesizer

You must be informed of the maximum ratings and operating instruction of all and each of the equipment used in the setup before using them. It is important to note that many of the devices implemented can be easily damaged by electrostatic discharges (ESD), exceeding maximum ratings or bad handling. Each of these devices has a proper instruction's manual or datasheet that has to be consulted.

The steps to use the system are as follows:

1. Connect the devices following diagram from Figure 3.6.
2. Disconnect the master laser from the system and turn it on. The laser needs three hours to stabilize.
3. Set the laser to the desired wavelength and set to power, ensuring that the input power is less than 30 mW.
4. Set the frequency synthesizer to the desired frequency and power and switch it on.
5. Connect the master laser to the input of the system.
6. Turn on the DC power supply and adjust the voltage to obtain the desired output.